Earth's Gravity Field to the Sixteenth Degree and Station Coordinates from Satellite and Terrestrial Data

E. M. GAPOSCHKIN AND K. LAMBECK[1]

Smithsonian Institution, Astrophysical Observatory
Cambridge, Massachusetts 02138

Geodetic parameters describing the earth's gravity field and the positions of satellite-tracking stations in a geocentric reference frame have been computed. These parameters were estimated by means of a combination of four different types of data: routine and simultaneous satellite observations, observations of deep-space probes, and measurements of terrestrial gravity. This combination solution gives better parameters than any subset of data types. In the dynamic solution, precision-reduced Baker-Nunn observations and laser range data of 21 satellites were used. Data from optical cameras, in addition to those from 19 Baker-Nunn stations, were used in the geometrical solution. Data from the tracking of deep-space probes were used in the form of relative station longitudes and distances to the earth's axis of rotation. The surface-gravity data in the form of mean anomalies for 300-n.mi. squares were provided by Kaula. The adopted solution from each iteration was a combination solution and was chosen to improve the residuals of all types of data. In addition to these four data sets, astrogeodetic data, surface triangulation, and some recently acquired surface-gravity data not included in the set used for the combinations were used for an independent test of the solution. The total gravity field is represented by spherical harmonic coefficients complete to degree and order 16, plus a number of higher-degree terms. The half-wavelength resolution of this global solution subtends about 11° at the earth's center. The accuracy of the global field has been estimated as ±3 meters in geoid height, or ±8.7 mgal. Coordinates of many of the stations are determined with an accuracy of 10 meters or better.

During 1966, the Smithsonian Astrophysical Observatory (SAO) published numerical parameters for the earth's gravity field and the coordinates of the satellite-tracking stations [*Gaposchkin*, 1967; *Köhnlein*, 1967*a*; *Veis*, 1967*a*, *b*; *Whipple*, 1967; *Lundquist and Veis*, 1966]. In 1967, a series of papers by Gaposchkin, Köhnlein, Kozai, and Veis [*Lundquist*, 1967] produced several refinements of the 1966 solution. Tests of the solution presented here indicate that these new results are superior to any set of geodetic parameters.

The geodetic parameters are estimated from a combined solution of the results obtained by the geometric and dynamic methods. In addition, the combination solution includes station-position information determined by the Jet Propulsion Laboratory (JPL) for its Deep Space Tracking Network (DSN) and surface-gravity anomalies computed by *Kaula* [1966*a*]. The final solution yields harmonic coefficients in the potential expansion complete to degree and order 16, plus 14 pairs of higher-degree coefficients and the coordinates for 39 stations. This solution is compared with recently available surface-gravity data and astrogeodetic data.

DATA COLLECTION, REDUCTION, AND REFERENCE SYSTEM

Data collection. Laser tracking systems have been developed in the past 4 years, and coordinated observing periods were established in 1967, 1968, and 1969. The best data include significant amounts of laser data.

In addition to data from the Baker-Nunn and laser networks, data collected by other agencies have also been used (see Figure 1):

1. Laser data from stations 7815, 7816, and 7818 were made available by the Centre National d'Etudes Spatiales (CNES), France.

2. Laser data from station 7050 were made available by the Goddard Space Flight Center (GSFC).

[1] Now at Observatoire de Paris, Meudon, France.

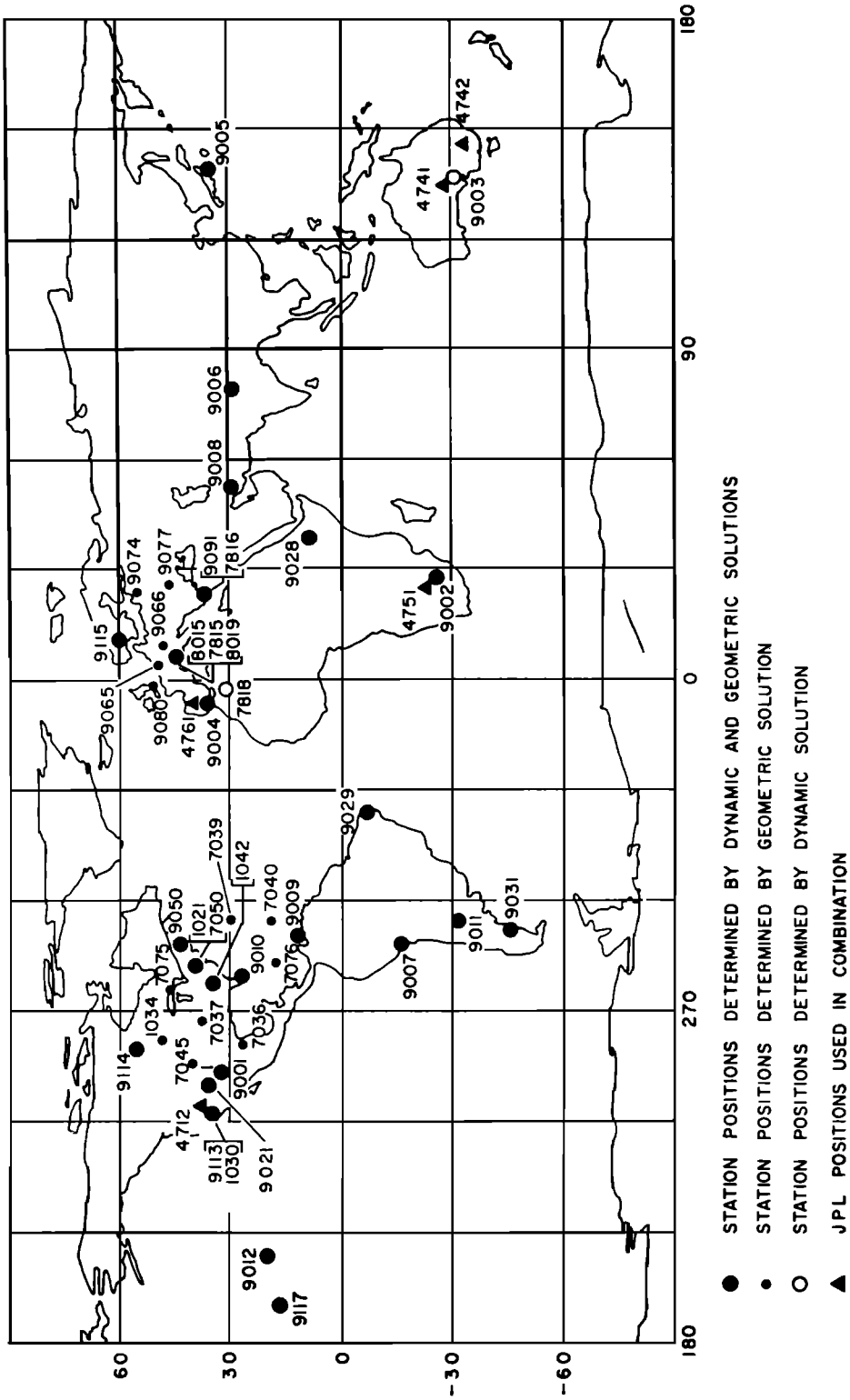

Fig. 1. Location of stations used. Collocated stations are bracketed together.

3. Optical data were obtained from the following European stations: 8015 and 8019 (Observatoire de Paris); 9065 (Technical University of Delft); 9066 (Astronomical Institute, Berne); 9074 and 9077 (USSR Astronomical Council); and 9080 (Royal Radar Establishment, Malvern).

4. Optical data from the MOTS cameras 1021, 1030, 1042, 7036, 7037, 7039, 7040, 7075, and 7076 were supplied by GSFC.

Data reduction and accuracies. The optical data were reduced with all terms in precession and nutation necessary to ensure that the maximum neglected effect is less than 0.5 meters. Annual aberration is added and diurnal aberration must be applied to the simultaneous observations. Parallactic refraction was applied by the use of mean nighttime temperature and pressure taken at each station to establish the refraction coefficient (G. Veis, private communication, 1966). Systematic corrections to star-catalog positions were applied where appropriate. All optical data received from other agencies were corrected in the same way. The accuracy of the optical data ranges from 1 to 4 arcsec [*Lambeck*, 1969*a*].

The laser range data are considered to be accurate to about 2 meters and are reduced by use of the corrections described by *Lehr* [1969]. The influence of timing errors at the stations has to be considered. For passes with more than 10 observed points, 10 points equally spaced in the pass are selected. To account for redundancy and systematic errors of the laser data, the assumed accuracy of each laser point is taken at 5 meters for the SAO and GSFC laser data and at 10 meters for the CNES data.

Reference system. SAO has its own master clock, and through VLF transmission maintains its own coordinated time system called A.S. The principal time reductions were to convert the GSFC data from UTC to A.S., and the CNES data from A3 to A.S. The UT1 data used in 1966 were a combination of final and preliminary values of the United States Naval Observatory (USNO). An examination of the differences between the USNO values and those of the Bureau International de l'Heure (BIH) revealed differences approaching 5 meters. For the present solution, BIH UT1 values have been adopted throughout. It appears that these data may be a limiting factor for the ultimately attainable accuracy of station positions. The polar-motion data were taken from the International Polar Motion Service (IPMS). The difference between these and the BIH data for the period since they were referred to the same origin is as much as 1.5 meters. The IPMS data used here were all referred to the mean pole of 1900–1905. The coordinate system used is the equator of date and the equinox of 1950.0. The choice of this system is discussed further in the next section. The position of the earth with respect to this system was tabulated in terms of the UT1 and polar-motion data.

As in 1966, the determination of the zonal harmonics was a precursor to this analysis. With use of the 1966 solution, the orbital information was completely revised. *Kozai's* [1969] zonal harmonics to J_{21} were used as starting values. The coefficients are listed for reference in Table 1. Also given are the adopted values for GM, a_e, and the velocity of light c.

DYNAMICAL SOLUTION

The main problem in celestial mechanics is to develop formulas (a theory in this nomenclature) that predict the trajectory when the forces and the initial conditions are established. In

TABLE 1. Adopted Zonal Harmonics to $J(21)$* and Other Constants

$J(2)$	1.08262800E-03
$J(3)$	−2.5380E-06
$J(4)$	−1.5930E-06
$J(5)$	−2.3000E-07
$J(6)$	5.0200E-07
$J(7)$	−3.6200E-07
$J(8)$	−1.1800E-07
$J(9)$	−1.0000E-07
$J(10)$	−3.5400E-07
$J(11)$	2.0200E-07
$J(12)$	−4.2000E-08
$J(13)$	−1.2300E-07
$J(14)$	−7.3000E-08
$J(15)$	−1.7400E-07
$J(16)$	1.8700E-07
$J(17)$	8.5000E-08
$J(18)$	−2.3100E-07
$J(19)$	−2.1600E-07
$J(20)$	−5.0000E-09
$J(21)$	1.4400E-07
GM	3.986013×10^{20} cm³/sec²
a_e	6.378155×10^{8} meters
c	2.997925×10^{10} cm/sec

* *Kozai*, 1969.

general, we must be satisfied with approximate solutions, which for our purpose are quite satisfactory. Alternatively, a direct numerical integration of the equations of motion could be carried out.

The forces we consider are the gravitational attraction of the earth, moon, and sun and the nongravitational effects of radiation pressure and air drag. In this analysis, we have chosen satellites that are dominated by the geopotential and for which other effects can, in some way, be assumed. *Kaula* [1966*b*] and *Gaposchkin* [1966*a*] describe detailed methods for orbital analysis. *Gaposchkin* [1968] discusses some considerations of this analysis, and further details are given by *Gaposchkin and Lambeck* [1970].

The gravity field of the earth, or equivalently, the geopotential, is quite irregular. The geopotential V can be represented as an infinite series of spherical harmonics, and the form adopted for this analysis is

$$V = \frac{GM}{r}\left[1 - \sum_{n=2}^{\infty} J_n\left(\frac{a_e}{r}\right)^n p_n(\sin\phi) + \sum_{l=2}^{\infty}\sum_{m=1}^{l}\left(\frac{a_e}{r}\right)^l P_{lm}(\sin\phi) \cdot (C_{lm}\cos m\lambda + S_{lm}\sin m\lambda)\right] \quad (1)$$

where GM is the product of the gravitational constant and the mass of the earth, ϕ and λ are earth-fixed latitude and longitude, a_e is the equatorial radius of the earth, and

$$p_n(\sin\phi) = \frac{1}{2^n}\sum_{k=0}^{r}(-)^k \frac{(2n-2k)!\sin^{n-2k}\phi}{k!\,(n-k)!\,(n-2k)!}$$

where r is the greatest integer $\leq n/2$,

$$P_{lm}(\sin\phi) = \left[\frac{2(2l+1)(l-m)!}{(l+m)!}\right]^{1/2}\frac{\cos^l\phi}{2^l} \cdot \sum_{k=0}^{r}(-)^k \frac{(2l-2k)!\sin^{l-m-2k}\phi}{k!\,(l-k)!\,(l-m-2k)!}$$

where r is the greatest integer $\leq (l-m)/2$. Expression 1 uses a mixed normalization. The expression P_{lm} $(\sin\phi)$ is the fully normalized associated Legendre polynomial, i.e.,

$$\int_{\text{sphere}} P_{lm}^2(\sin\phi)\begin{Bmatrix}\sin m\lambda\\ \cos m\lambda\end{Bmatrix}^2 d\sigma = 4\pi \quad m \neq 0$$

and C_{lm}, S_{lm} are fully normalized coefficients, as previously published (sometimes designated as $\bar{C}_{lm}$, $\bar{S}_{lm}$). The p_n $(\sin\phi)$ are the conventional Legendre polynomials, and the J_n are conventional harmonics. To include the J_n in the fully normalized form, we have

$$P_{l,0} = (2l+1)^{1/2}p_l$$

$$C_{l,0} = -J_l/(2l+1)^{1/2}$$

and the summation in equation 1 would be $m = 0, 1, 2, \cdots, l$. The C_{lm}, S_{lm} are called tesseral harmonics, and the J_n are called zonal harmonics. For a systematic development, see *Heiskanen and Moritz* [1967].

In equation 1, we assume $J_1 = C_{21} = S_{21} = 0$ because the origin of the coordinate system chosen is referred to the earth's center of mass, and the z axis ($\phi = \pi/2$) is along the principal axis, i.e., the axis of maximum moment of inertia. In fact, these are only assumptions and one can only approximately realize such a coordinate system.

The tesseral harmonics are determined from the short-period (1 revolution to 1 day) changes in the orbit. The detailed structure of the orbit must be observed, and each observation provides an observation equation. Data of the highest possible precision are needed.

Apart from the resonant harmonics, the terms higher than $l = 12$, $m = 12$ are weakly determined by the satellite data (when the satellite is low, it is infrequently observed), but it had been demonstrated in early iterations that the surface gravity could determine these higher harmonics. The satellite solution was limited to those harmonics that have an effect of greater than 3 to 4 meters on the orbit. The resulting terms were complete through $l = 12$, $m = 12$, omitting $C/S(11, 7)$, $C/S(12, 6)$, and $C/S(12, 9)$. Higher-order terms selected were $C/S(l, 1)$ $13 \leq l \leq 16$; $C/S(l, 2)$ $13 \leq l \leq 15$; $C/S(14, 3)$; $C/S(l, 12)$ $13 \leq l \leq 19$; $C/S(l, 13)$ $13 \leq l \leq 21$; $C/S(l, 14)$ $14 \leq l \leq 22$. The $m = 9, 12, 13, 14$ terms are resonant with some satellites. *Gaposchkin and Lambeck* [1970, Table 4] list the resonant satellites with their

resonant periods. Several satellites are resonant with more than one order. The stations were restricted to those observing many satellites. Other stations were more appropriately determined by the geometric solution.

Table 2 details the selection of satellites used in the final solution, ordered by inclination. Figure 2 indicates the distribution of satellites, many of which were not used in the 1966 solution. The selection of data and unknowns evolved through the analysis. The number of satellites used ranged from 21 to 25, and the number of arcs in the largest solution was 244. Arcs were added and rejected on the basis of contribution to the normal equations, number of observations for a particular station, improvement of distribution for a resonant harmonic, and quality of the orbital fit.

GEOMETRIC SOLUTION

The geometric method for determining station positions from observations of satellites does not require any knowledge of the orbit, since the object is observed simultaneously from two or more stations and the relative positions of these stations are computed by a three-dimensional triangulation process. The geometric solution does not give any information on the position of the earth's center of mass, nor does it give a scale determination if only direction observations are used. The solution is further characterized by highly accurate directions between stations, but also by an unfavorable error propagation in station coordinates. When combined with the dynamic solution, the geometric solution contributes significantly to the solution for station coordinates and provides a valuable means of assessing the reliability of these results.

A total of 38 stations was involved in this solution, and 20 of these were also used in the dynamic solution. Observations from 16 SAO and 4 United States Air Force (USAF) Baker-Nunn cameras, from 13 National Aeronautics and Space Administration (NASA) MOTS cameras, and from 7 European stations were utilized. Approximately 50,000 individual direction observations were used in the analysis, a number comparable to that used in the dynamic solution. The distribution of the data among the stations is given by *Gaposchkin and Lambeck* [1970, Table 6]. Most of the observations have been made to high-altitude satellites not used in the dynamic solution. These satellites include 6102801 (Midas 4), 6303004, 6605601 (Pageos), and 6805501. For stations

TABLE 2. Summary of Dynamical Data

Satellite	Name or Other Designation	Inclination, deg	Eccentricity	Semimajor Axis, km	Perigee Height, km	Number of Arcs	Days/Arc	New Satellite	Select Files	Laser Data
6001301	Courier 1B 60 ν1	28	0 016	7465	965	6	30	×	×	
5900101	Vanguard 2 59 α1	33	0.165	8300	557	7	30		×	
6100401	61 δ1	39	0.119	7960	700	3	14			
6701401	D1D	39	0 053	7337	569	6	14	×	×	×
6701101	D1C	40	0.052	7336	579	4	14	×	×	×
6503201	Explorer 27 BE-C	41	0.026	7311	941	4	30	×	×	×
6000902	60 ι2	47	0.011	7971	1512	7	30			
6206001	Anna 1B 62 $\beta\mu$1	50	0 007	7508	1077	12	30		×	
6302601	Geophysical Research	50	0 062	7237	424	6	14			
6508901	Explorer 29 Geos 1	59	0.073	8074	1121	21	30	×	×	×
6101501	Transit 4A 61 o1	67	0 008	7318	885	8	30			
6101502	Injun 1 61 o2	67	0.008	7316	896	4	30			
6506301	Secor 5	69	0 079	8159	1137	2	30	×	×	
6400101		70	0.002	7301	921	3	30	×		
6406401	Explorer 22 BE-B	80	0 012	7362	912	2	30	×		×
6508101	Ogo 2	87	0.075	7344	420	2	14	×		
6600501	Oscar 07	89	0.023	7417	868	1	30	×	×	
6304902	5BN-2	90	0.005	7473	1070	5	30	×		
6102801	Midas 4 61 $\alpha\delta$1	96	0.013	10005	3503	3	50			
6800201	Explorer 36 Geos 2	106	0.031	7709	1101	6	14	×		×
6507801	OV1 2	144	0.182	8306	416	2	14	×		
						114				

closer than about 2500 km, observations in both the passive and the flashing modes of 6508901 (Geos 1) and 6800201 (Geos 2) form the majority of the data.

The Baker-Nunn network is used here as the basic global framework in the adjustment, but because of the station distribution this net is best considered in two parts: the American-Pacific stations (group 1) and the Afro-Eurasian stations (group 2). These two groups link up at San Fernando (9004), at Tokyo (9005), and to a lesser extent at Oslo (9115), so that all the SAO stations with the exception of Woomera (9023) can be connected into one net.

Independent adjustments for the stations in these two groups, as well as for a third group comprising the MOTS data from North America and a fourth comprising data from the European stations, were performed. This subdivision was made in order to isolate and detect possible systematic errors arising from different reduction techniques or instrumentation used in the different data sources and to separate the propagation of variances caused by the poor geometry provided by the station positions from the propagation of the variances of the observed quantities.

Then the four groups of stations were linked via common stations. In linking the groups, it was necessary to determine only the relative translations and scale. No differential rotations needed to be considered, since all the data used in this analysis refer to the same astronomical reference system, polar-motion data, and UT1.

These adjustments were made by a least-squares procedure, carrying along the full covariance matrices of the functions of the observed quantities from step to step. Such a procedure

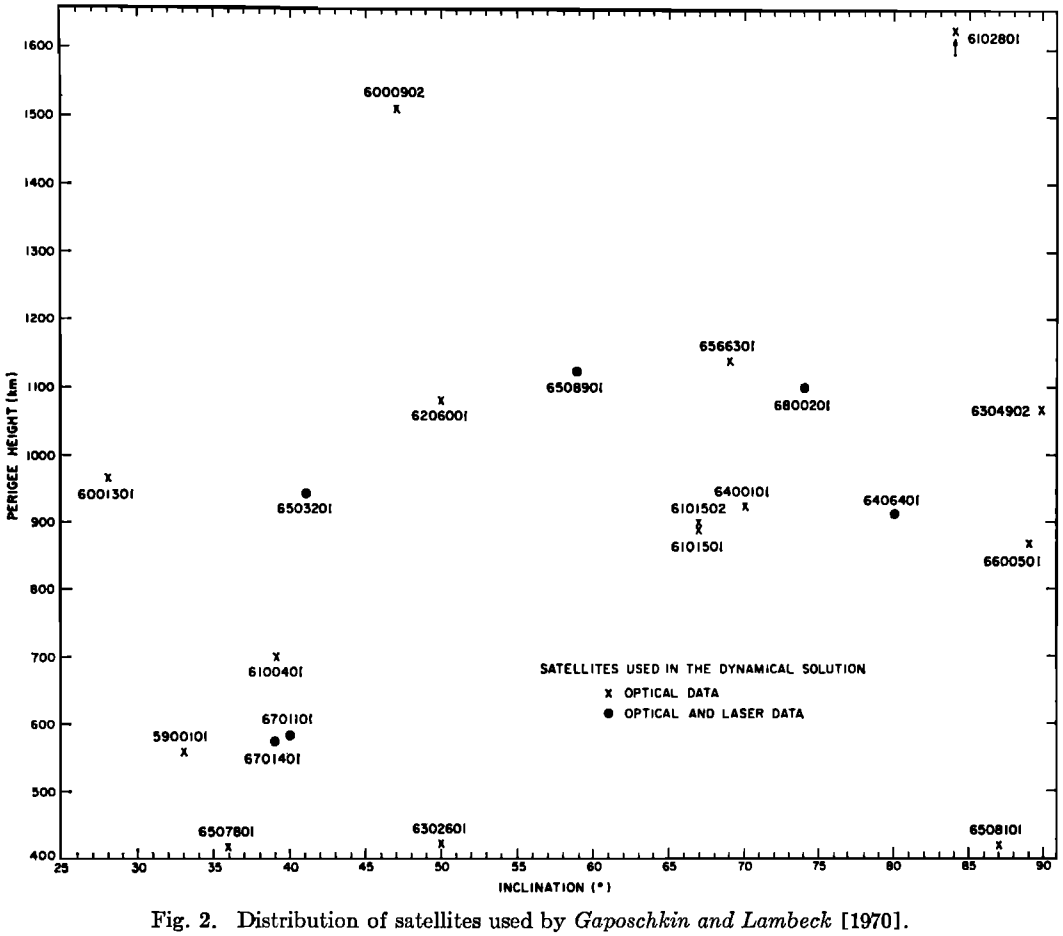

Fig. 2. Distribution of satellites used by *Gaposchkin and Lambeck* [1970].

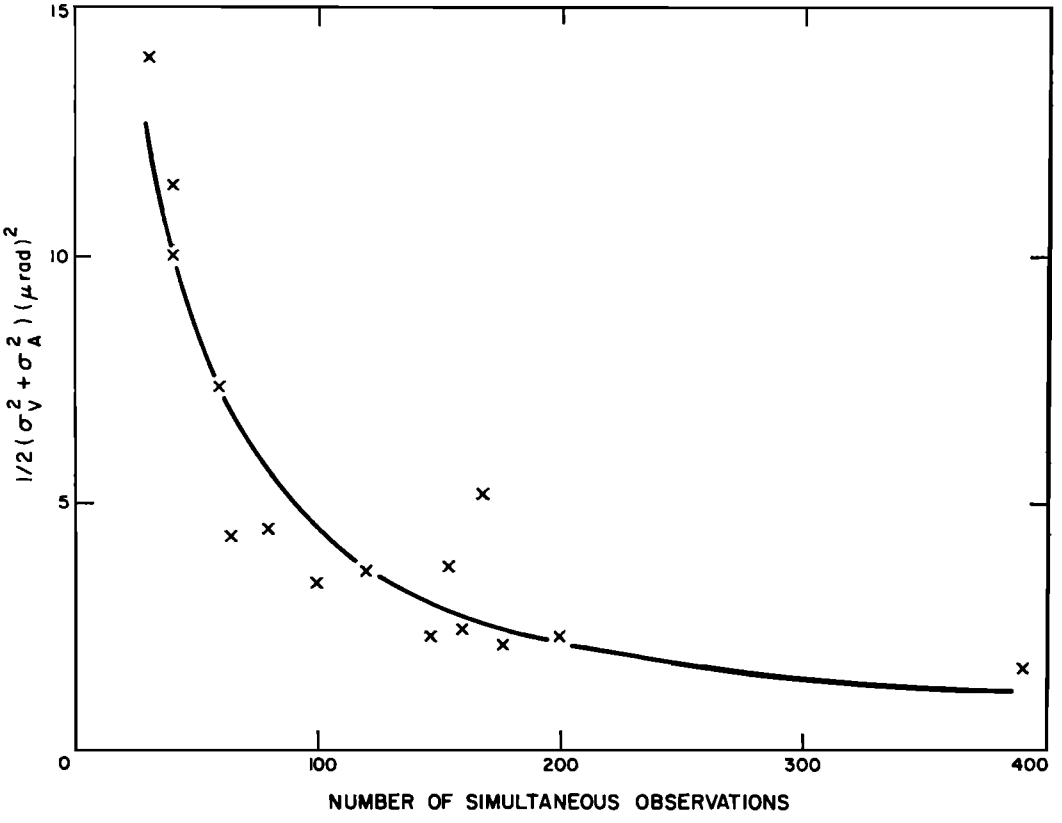

Fig. 3. Mean accuracy of station-station vector as a function of the number of pairs of simultaneous observations used. The crosses mark results obtained from the analysis, and the solid line indicates the expected results for the ratio (station-station distance)/satellite height = 1.2. The accuracy of a synthetic observation is 7 μrad (1.5 arcsec).

is equivalent to adjusting all the data in a single step [*Tienstra*, 1956; *Baarda*, 1967], but it has the advantage of isolating possible systematic errors in the data. If statistical testing of the results indicated the presence of such errors, the adjustments were further split up in an attempt to locate the faulty data. The statistical testing procedures used followed the ideas of *Baarda* [1968].

Throughout the adjustment, it has been assumed that observations taken at different time instants or from different stations are uncorrelated. Systematic timing errors may prevail over a long period, so that the first assumption is difficult to justify. The second assumption, however, appears generally acceptable, since error in time kept at distant stations is almost always uncorrelated. An analysis of the results of the adjustment of the various steps will indicate whether or not these assumptions are valid.

For the single station-station vector adjustments, the average variance factor is 1.5 and varies from 0.7 to 3.1 [*Gaposchkin and Lambeck*, 1970, Table 7]. If no systematic errors are present, the expected value of this quantity should be unity. For example, station-station vectors associated with station 9028 consistently show a large variance factor, indicating possible systematic errors in data from this station. The accuracies of the station-station vectors vary between 0.2 and 2 arcsec, depending on the number of observations and the station-satellite geometry. Figure 3 is a plot of the accuracies for vectors between SAO Baker-Nunn cameras for which the number of simultaneous events is greater than 30. Also shown are the expected accuracies given by the expression [*Lambeck*,

1969b]

$$\begin{bmatrix} \sigma_V^2 \\ \sigma_A^2 \end{bmatrix} = \frac{\sigma_S^2}{n} \begin{bmatrix} 1/[0.09(L/h) - 0.03] \\ 1/[0.34(L/h) - 0.15] \end{bmatrix}$$

where σ_S is the accuracy of a synthetic observation (1.5 arcsec), and L/h is the average ratio of length of station-station vector to satellite height (≈ 1.2); σ_V is the accuracy in the vertical component, and σ_A is the accuracy in the azimuth component of the station-station vector, and generally the correlation between these components is small.

The variances of unit weight for the adjustment in the second phase of the four groups of stations are the following:

group 1 $\sigma_1^2 = 1.39$ (Baker-Nunn, Americas, Pacific, Atlantic).
group 2 $\sigma_2^2 = 1.59$ (Baker-Nunn, Afro-Eurasian).
group 3 $\sigma_3^2 = 0.93$ (European Optical).
group 4 $\sigma_4^2 = 1.99$ (North American MOTS).

Application of the variance ratio tests to the results leads to the general conclusion that, with the exception of the data in group 3, the null hypothesis (i.e., there are no model errors) is to be rejected. However, a reevaluation of the original data gave no indication where the problems may occur, and the results have, of necessity, been accepted.

Finally, the adjustment linking the four groups of data gives a variance of unit weight equal to 1.4 with 16 degrees of freedom and $F_{0.95,16,\infty} = 1.71$. This suggests that the observations and methods of reduction used in the four groups are compatible.

To investigate further the unsatisfactory conclusions that have to be drawn from the independent group adjustments, the directions between stations were computed from the linked adjustment results and were compared with the independent group station-station vectors (see *Gaposchkin and Lambeck* [1970, Figure 4] for some examples). Both these vectors represent estimates of the same quantity, and they can be expected to lie within the accuracy estimates given for them. Comparisons for all the station-station vectors show that this is the case about 60% of the time.

Denoting the mean accuracy of a station-station vector derived from phase 1 by σ_1 and that derived from phase 3 by σ_2, and denoting the angular distance between the two estimates of the vector by δ, we would expect that on the average

$$\delta^2 \leq (1/2)(\sigma_1^2 + \sigma_2^2)$$

These quantities are given by *Gaposchkin and Lambeck* [1970, Table 7], and their values, averaged over the vectors used, indicate that this condition is not satisfied unless the variance estimates are multiplied by a factor

$$k^2 = \frac{\delta^2}{(1/2)(\sigma_1^2 + \sigma_2^2)}$$

These results yield a value of $k^2 = 2.8$, and the covariance matrix for the final geometric solution is multiplied by this number. The final directions between stations are given by *Gaposchkin and Lambeck* [1970, Table 8].

Information from Deep-Space Probes

The DSN has used data from its tracking of deep-space probes to obtain, among other parameters, the relative longitudes and the distances to the earth's axis of rotation of their antennas [*Vegos and Trask*, 1967; *Trask and Vegos*, 1968]. As the JPL sites can be related to nearby Baker-Nunn sites, by use of ground-survey information, a valuable and completely independent control of the results is possible. Comparison with the JPL data is particularly important for the two instances where the geometric solution is either very poor (South Africa) or nonexistent (Australia). The two sets of data also complement each other, since the JPL solution gives a very strong scale and relative longitude determination but no latitude information, whereas the SAO solution accurately determines the orientation with respect to the astronomical reference system.

The JPL and SAO results were compared by *Veis* [1966] and *Vegos and Trask* [1967] using data from the Ranger missions. However, more refined JPL solutions have recently become available using data from the Mariner 4 and 5 missions. The solution used in the present analysis is that of *Mottinger* [1969], called LS 25. Table 3 gives his determination for the station locations. Mottinger estimates the standard deviations of the computed quantities to be about 3 meters. In this solution, the polar-

TABLE 3. Locations of the JPL Antennas*

Station	λ, deg	r_s, km	X, km	Y, km
4712	243.194559	5212.0535	−2350.4397	−4651.9819
4741	136.887507	5450.1986	−3978.7174	3724.8454
4742	148.981301	5205.3504	−4460.9809	2682.4097
4751	27.685432	5742.9417	5085.4425	2668.2678
4761	355.751007	4862.6078	4849.2429	− 360.2752

* Determined by *Mottinger* [1969].

motion data from BIH and UT1 derived from USNO data are used. Thus, a difference in longitude between the JPL and the SAO solution can be expected. A longitude difference can also arise from possible discrepancies in the right-ascension definitions of the planetary ephemeris used by JPL and of the star catalog used at SAO.

The geodetic coordinates of the JPL and associated Baker-Nunn stations are given by *Gaposchkin and Lambeck* [1970, Table 10]. In three cases, 9002-4751 (South Africa), 9003-4741 (Australia), and 9113-4712 (United States), the survey distance between the stations is small and any datum tilts or distortions should not cause problems when the geodetic survey information is used to relate the two earth-centered systems. However, for the other two JPL-SAO station groups, 9003-4742 and 9004-4761, this may not be true, and corrected survey differences have been computed on the basis of the datum adjustments of the European and Australian datums [*Lambeck*, 1970, 1971*a*].

SURFACE-GRAVITY DATA

Surface-gravity data provide a means of comparing the satellite solution with an external standard and of improving the over-all gravity-field solution. The satellite solutions are most suited for determining the lower-order harmonics, while the surface-gravity data are expected to contribute most to the higher-order terms. The dynamic satellite solution described above gives a complete representation to degree and order 12, with the exception of the (11, 7), (12, 6), and (12, 9) harmonics; and for higher degrees only those coefficients with orders 1, 2, 3 and 12, 13, 14 have been determined from the present data. The surface gravity, on the other hand, does not reflect such a partiality to certain coefficients, and all terms of the same degree can be determined with about equal reliability.

The gravity anomalies Δg can be related to the harmonic coefficients by

$$\Delta g = \gamma \sum_{l=2}^{\infty} \sum_{m=0}^{n} (l-1)\left(\frac{a}{r}\right)^{l} \cdot (C_{lm} \cos m\lambda + S_{lm} \sin m\lambda) P_{lm}(\sin \phi)$$

where $C_{2,0}$ and $C_{4,0}$ are referred to a specified reference ellipsoid, in this case $f = 1/298.258$, corresponding to *Kozai*'s [1969] determination for J_2. Thus, if Δg is known all over the earth, the harmonic coefficients can be estimated. This approach was used by *Köhnlein* [1967*b*] and is also used here. (The flattening f is a derived quantity, depending upon a_e among other things. Using $a_e = 6.378155$, the value adopted for this analysis is $f = 1/298.257$. A better value (see next section or *Lambeck* [1971*a*]), $a_e = 6.378140$, gives $f = 1/298.258$. The formulas for f are taken from *Cook* [1959].)

No serious attempt has been made to determine estimates of the zonal harmonics from the surface-gravity data because of their poor distribution, particularly at the southern latitudes.

Data prepared by *Kaula* [1966*a*] were used in this analysis. His basic data consisted of 1° × 1° mean free-air anomalies computed essentially by the techniques described by *Uotila* [1960]. These anomalies were combined to form mean values for areas of 60 × 60 ± 30 n.mi. (nautical miles) in order to obtain a set as nearly statistically uniform as possible. To obtain estimates for 300-n.mi. squares, Kaula next estimated 60-n.mi. area anomalies for the unsurveyed areas applying linear regression methods [*Kaula*, 1966*c*] to the 60-n.mi. means within the 300-n.mi. area. Finally, he computed

the 300-n.mi. means as the arithmetic mean of all the observed and extrapolated 60-n.mi. means within the area. The results were 935 mean anomalies for 300-n.mi. squares covering 56.5% of the globe and are given by *Gaposchkin and Lambeck* [1970, Table 12].

For the remaining 43.5% of the globe, three alternative assumptions were made in the present analysis:

1. No assumptions were made about these areas and only the observed anomalies were used.
2. The model anomalies generated by Kaula from a linear regression analysis of his 935 observed squares [*Kaula*, 1966*d*] were used.
3. The anomalies were set to zero and a large variance was used.

Kaula used for the variance of each 300-n.mi. square

$$\sigma_{g_i}^2 = g_T^2/(n_i + 1)$$

where $g_T^2 = 274$ mgal^2 is the mean value of the square of the gravity anomaly, and n is the number of observed 60-n.mi. areas contained in the 300-n.mi. square.

However, the several assumptions made in computing the gravity anomaly by linear regression may make this variance too small. The most important assumption made is the one restricting the regression analysis to points within the 300-n.mi. square and ignoring possible correlations of gravity with topography. Consequently, in the present analysis the above variance estimates have been multiplied by a factor of 4. In the analyses of earlier iterations of the combination solution, this factor was found to give a set of potential coefficients that improved both the satellite orbits and the surface-gravity comparison. With this variance, a 300-n.mi. square with a surveyed 60-n.mi. area receives a standard deviation of 23 mgal, while a completely surveyed 300-n.mi. area (twenty-five 60-n.mi. squares) receives a standard deviation of 6.5 mgal.

Some screening of the surface-gravity data was done by comparing the gravity anomalies from the combination solution in any one iteration with the surface-gravity data and rejecting an anomaly using a three-sigma criterion. This does not necessarily imply an error in the surface-gravity data, but it could mean that the rejected anomaly represents a short-wavelength variation that is not reflected in the satellite solution.

In the final solution, 38 anomalies were rejected. Of these, five were squares with $n \geq 10$ and one was a square with $n \geq 20$.

More recent surface-gravity compilations have been published by *Talwani and Le Pichon* [1969] and *Le Pichon and Talwani* [1969] for the Atlantic and Indian oceans. These new data have been used for comparisons with the new satellite combination solutions given here.

A comparison of results obtained using the different assumptions about the surface gravity in the unsurveyed areas indicates no difference between the anomaly set derived from regression analysis and the set of zero anomalies. This may have been expected, since g_T^2 for the predicted anomalies is only 121 mgal^2, very much less than either the $g_T^2 = 274$ mgal^2 for the observed squares or the variances associated with the predicted values (30 mgal)^2.

However, these two tests did show a difference in results from the one that ignored the unsurveyed areas altogether. This difference occurred in those extensive areas in southern latitudes where there were no surface data and where the station distribution was unfavorable. The effect of using the model anomalies was to reduce by about 5 meters the heights of the major geoid features in these areas. In the other areas, the differences in geoid heights did not exceed 2 meters.

COMPARISONS AND COMBINATION SOLUTION

Data from the various sources can now be combined to determine a consistent set of geodetic parameters of the earth. All four methods discussed in the preceding sections are incomplete in one way or another, and the inadequacies in the mathematical models used will lead to unrealistic accuracy estimates. Consequently, the data from the different sources serve two purposes: one of comparison, to obtain realistic accuracy estimates and to resolve any biases in the results; and one of combination, to obtain the most complete and reliable set of geodetic parameters.

Combination solution. In combining the two satellite solutions, it must be remembered that the geometric solution is essentially unscaled and its origin is arbitrarily determined, so that, in

the transformation linking it to the dynamic solution, three translation and one scale parameters must be introduced. A rotation term is also introduced to determine whether a systematic longitude discrepancy exists between these two solutions. Such a term could conceivably arise from correlations that exist in the dynamic solution among longitude, time, and right ascension of the node.

The JPL solution of *Mottinger* [1969] is combined with the satellite solution by introducing a second longitude rotation and a second scale parameter. The need for the former has been discussed above, and the latter was intro-

TABLE 4. Geocentric Coordinates of the Stations Determined in the Final Combination Solution

Station	X, Mm	Y, Mm	Z, Mm	σ^*, meters	Station Name
1021	1.118029	−4.876316	3.942984	7	Blossom Point, Md.
1034	−.521702	−4.242049	4.718731	7	Grand Forks, Minn.
1042	.647515	−5.177924	3.656707	7	Rosman, N. C.
7036	−.828496	−5.657458	2.816812	7	Edinburg, Tex.
7037	−.191286	−4.967280	3.983262	7	Columbia, Mo.
7039	2.308239	−4.873597	3.394580	10	Bermuda
7040	2.465067	−5.534924	1.985510	10	Puerto Rico
7045	−1.240479	−4.760229	4.048995	9	Denver, Col.
7050	1.130674	−4.831368	3.994111	7	Goddard Space Flight Center
7075	.692628	−4.347059	4.600483	9	Sudbury, Ont.
7076	1.384174	−5.905685	1.966533	10	Jamaica
7815	4.578370	.457951	4.403134	5	Haute Provence, France
7816	4.654337	1.959134	3.884366	5	Stephanion, Greece
7818	5.426329	−.229330	3.334608	15	Colomb-Bechar, Algeria
7901	−1.535757	−5.166996	3.401042	5	Organ Pass, N. M.
8015	4.578328	.457966	4.403179	5	Haute Provence, France
8019	4.579466	.586599	4.386408	5	Nice, France
9001	−1.535757	−5.166996	3.401042	5	Organ Pass, N. M.
9002	5.056125	2.716511	−2.775784	7	Pretoria, S. Africa
9003	−3.983776	3.743087	−3.275566	6	Woomera, Australia
9004	5.105588	−.555228	3.769667	5	San Fernando, Spain
9005	−3.946693	3.366299	3.698832	10	Tokyo, Japan
9006	1.018203	5.471103	3.109623	9	Naini Tal, India
9007	1.942775	−5.804081	−1.796933	7	Arequipa, Peru
9008	3.376893	4.403976	3.136250	9	Shiraz, Iran
9009	2.251829	−5.816919	1.327160	7	Curaçao, Antilles
9010	.976291	−5.601398	2.880240	5	Jupiter, Fla.
9011	2.280589	−4.914573	−3.355426	9	Villa Dolores, Argentina
9012	−5.466053	−2.404282	2.242171	7	Maui, Hawaii
9021	−1.936782	−5.077704	3.331916	15	Mt. Hopkins, Ariz.
9023	−3.977766	3.725102	−3.303035	6	Island Lagoon, Australia
9025	−3.910437	3.376361	3.729217	10	Dodaira, Japan
9028	4.903750	3.965201	.963872	12	Addis Ababa, Ethiopia
9029	5.186461	−3.653856	−.654325	12	Natal, Brazil
9031	1.693803	−4.112328	−4.556649	15	Comodoro Rivadavia, Argentina
9050	1.489753	−4.467478	4.287304	14	Harvard, Mass.
9065	3.923411	.299882	5.002945	12	Delft, Holland
9066	4.331310	.567511	4.633093	7	Zimmerwald, Switzerland
9074	3.183901	1.421448	5.322772	10	Riga, Latvia
9077	3.907421	1.602397	4.763890	10	Uzghorod, USSR
9080	3.920178	−.134738	5.012708	9	Malvern, England
9091	4.595157	2.039425	3.912650	5	Dioysos, Greece
9113	−2.450011	−4.624421	3.635035	7	Rosamund, Cal.
9114	−1.264838	−3.466884	5.185467	12	Cold Lake, Canada
9115	3.121280	.592643	5.512701	17	Harestua, Norway
9117	−6.007402	−1.111859	1.825730	15	Johnston Isl., Pacific

* Formal precision estimates of the coordinates.

duced to absorb possible biases in either solution that have the characteristic of a scale error. In theory, this scale factor should be zero, since both SAO and JPL have used the same value for GM, but 'pseudo' scale errors could be introduced. For example, a systematic error in the refraction corrections to Baker-Nunn observations could have an effect similar to a scale error.

In combining the JPL solution with the other data, the normalized covariance matrix supplied by Mottinger was used. This matrix was scaled by his accuracy estimates for the components of the station positions and preserves the strong correlation that exists between the longitudes of the solution.

The results from the surface-gravity analysis can be directly related to the combined solution, since both refer to the same reference ellipsoid and GM. The zonal harmonics derived by Kozai have not been included in this combination, since his solution is quite independent of the satellite analysis of the tesseral harmonics, and the surface-gravity data, because of their poor distribution, do not contain any significant zonal information.

The final combination solution contains a total of 424 unknowns, 117 station coordinates, 296 harmonic coefficients, and 11 scale, rotation, and translation parameters. In a solution of this kind, several iterations were made (as described above), and several alternative weighting schemes were considered. These weight factors are used to scale the covariance matrices derived for the individual solutions and in the combination. As was already indicated, the covariance matrix of the geometric solution has been multiplied by 2.8, and the covariance matrix of the surface-gravity results by 4.0. The covariance matrix of the dynamical solution has been multiplied by 4.5 for the reasons described in the next section, whereas, for the JPL results, the accuracy estimates of Mottinger have been adopted without any further modification. This weighting scheme gives the best agreement in the tests described in the next section. The final results for station coordinates are presented in Table 4, and for harmonic coefficients in Table 5.

The power spectrum

$$\sigma_l^2 = (1/n_l) \sum_{m=0}^{l} (C_{lm}^2 + S_{lm}^2)$$

TABLE 5. Fully Normalized Coefficients of the Spherical Harmonic Expansion of the Geopotential Obtained in the Final Iteration of the Combination Solution

(C_{lm} are the cosine terms of degree l and order m, and S_{lm} are the sine terms.)

l	m	C_{lm}	S_{lm}
2	2	2.4129E-06	−1.3641E-06
3	1	1.9698E-06	2.6015E-07
3	2	8.9204E-07	−6.3468E-07
3	3	6.8630E-07	1.4304E-06
4	1	−5.2989E-07	−4.8765E-07
4	2	3.3024E-07	7.0633E-07
4	3	9.8943E-07	−1.5467E-07
4	4	−7.9692E-08	3.3928E-07
5	1	−5.3816E-08	−9.7905E-08
5	2	6.1286E-07	−3.5087E-07
5	3	−4.3083E-07	−8.6663E-08
5	4	−2.6693E-07	8.3010E-08
5	5	1.2593E-07	−5.9910E-07
6	1	−9.8984E-08	3.7652E-08
6	2	5.4825E-08	−3.5175E-07
6	3	2.7873E-08	4.4626E-08
6	4	−4.0342E-10	−4.0388E-07
6	5	−2.1143E-07	−5.2264E-07
6	6	8.8693E-08	−7.4756E-08
7	1	2.4142E-07	1.1567E-07
7	2	2.8306E-07	1.5645E-07
7	3	2.0285E-07	−2.3448E-07
7	4	−1.9727E-07	−1.1390E-07
7	5	−8.7024E-10	9.8461E-08
7	6	−2.5847E-07	1.0209E-07
7	7	1.5916E-07	−6.7710E-08
8	1	3.1254E-08	2.5696E-08
8	2	4.8161E-08	8.4140E-08
8	3	−5.7444E-08	1.8086E-08
8	4	−1.5378E-07	7.5264E-08
8	5	−5.6733E-08	6.1636E-08
8	6	−5.3903E-08	2.5930E-07
8	7	3.4390E-08	8.9168E-08
8	8	−7.7364E-08	6.7607E-08
9	1	1.3823E-07	−1.6100E-08
9	2	6.6741E-09	−8.1733E-08
9	3	−9.6463E-08	−1.1817E-07
9	4	5.7125E-08	1.1183E-07
9	5	−6.1435E-09	3.3551E-09
9	6	2.4186E-08	2.2028E-07
9	7	−5.0450E-08	−1.2700E-07
9	8	2.3359E-07	5.7239E-08
9	9	−8.2490E-08	9.2326E-08
10	1	1.1251E-07	−1.0167E-07
10	2	−3.1225E-08	−1.0450E-07
10	3	−2.3346E-08	−1.4137E-07
10	4	−4.8185E-08	−4.3248E-08
10	5	−8.0004E-08	−1.4279E-07
10	6	−3.2486E-08	−2.0153-0E7
10	7	5.4961E-08	3.2003E-08
10	8	7.3957E-08	−7.9706E-08
10	9	−6.8563E-09	6.2498E-09
10	10	1.2377E-07	−2.5885E-08
11	1	4.3900E-09	2.9751E-08

TABLE 5 (*continued*)

l	m	C_{lm}	S_{lm}
11	2	4.8900E-08	−9.1994E-08
11	3	−6.3247E-08	−1.3109E-07
11	4	−3.0193E-08	5.4317E-08
11	5	3.2523E-08	1.3215E-07
11	6	3.7517E-08	6.9005E-09
11	7	4.5726E-08	−1.3862E-07
11	8	6.4546E-08	−1.6993E-08
11	9	1.1750E-07	−9.9451E-09
11	10	−1.1736E-07	−1.8900E-08
11	11	1.1785E-07	−4.0688E-08
12	1	−4.5955E-08	−3.1000E-08
12	2	2.7481E-08	7.5986E-08
12	3	5.8386E-08	5.4784E-08
12	4	−4.3649E-08	−2.2262E-08
12	5	2.3375E-08	4.2637E-08
12	6	−2.3868E-08	−6.6770E-10
12	7	1.4507E-08	9.9784E-08
12	8	−5.7854E-09	3.3752E-08
12	9	−3.2232E-08	4.2858E-08
12	10	−1.8590E-08	4.8382E-09
12	11	−4.4921E-08	−4.8206E-08
12	12	−1.9407E-08	−5.7771E-08
13	1	−5.6042E-08	2.6288E-08
13	2	−4.7456E-08	1.7367E-08
13	3	2.3833E-08	−2.8930E-08
13	4	−1.9980E-08	5.7030E-08
13	5	9.6637E-08	−4.7760E-08
13	6	−8.3417E-08	5.9782E-08
13	7	−5.2217E-08	−3.2562E-09
13	8	−4.1759E-08	−2.0231E-08
13	9	−2.5623E-08	1.0767E-07
13	10	8.6589E-08	−1.0528E-08
13	11	−3.3749E-08	5.8541E-08
13	12	−1.3229E-09	8.2192E-08
13	13	−7.0288E-08	7.4643E-08
14	1	−2.3090E-08	4.9664E-08
14	2	3.2120E-08	−4.5289E-08
14	3	1.9042E-08	1.1919E-09
14	4	7.8017E-09	−3.7527E-08
14	5	−2.5958E-08	−2.3344E-08
14	6	1.9140E-08	−5.8721E-08
14	7	1.1061E-08	8.4132E-09
14	8	−3.0273E-08	−6.0838E-08
14	9	4.9539E-08	9.2345E-08
14	10	5.3732E-08	−4.3168E-08
14	11	2.7833E-08	−8.1637E-08
14	12	1.2481E-08	−5.7314E-08
14	13	5.1554E-08	4.5453E-08
14	14	−5.2082E-08	−1.2840E-08
15	1	−3.5971E-09	4.0142E-08
15	2	−4.4833E-08	−1.6056E-08
15	3	8.3016E-09	−5.7218E-09
15	4	1.3916E-08	6.6644E-08
15	5	3.1684E-08	1.8250E-09
15	6	7.0020E-08	−1.1872E-07
15	7	1.1856E-07	4.2690E-08
15	8	−9.7657E-08	−3.5710E-08
15	9	2.2064E-08	2.6632E-08
15	10	−2.0648E-08	5.3724E-10

TABLE 5 (*continued*)

l	m	C_{lm}	S_{lm}
15	11	−3.2585E-08	9.4052E-08
15	12	1.0524E-08	6.8726E-09
15	13	−3.7348E-08	4.0249E-09
15	14	1.2193E-08	−2.6786E-08
15	15	1.4515E-09	−1.4802E-08
16	1	−2.3789E-08	7.6413E-08
16	2	2.1327E-08	3.0669E-08
16	3	−4.7358E-08	3.2610E-08
16	4	−1.1591E-08	4.3001E-08
16	5	−4.4201E-08	3.2230E-08
16	6	−5.8439E-08	−4.2809E-08
16	7	1.0591E-07	8.1008E-09
16	8	−8.4738E-08	−2.4677E-09
16	9	9.0001E-09	−1.0628E-07
16	10	−2.9849E-08	−5.2467E-10
16	11	6.8502E-09	−7.0765E-08
16	12	2.2834E-08	−3.4087E-08
16	13	3.5475E-08	2.0683E-08
16	14	−7.3590E-09	−2.2626E-08
16	15	−3.5485E-08	8.4126E-10
16	16	−2.9522E-08	8.6217E-09
17	12	8.3097E-08	3.5424E-09
17	13	3.2749E-08	4.2920E-10
17	14	−1.6058E-08	2.7286E-08
18	12	1.1662E-08	8.4724E-09
18	13	4.6903E-09	−3.5547E-08
18	14	−2.7446E-08	−4.8376E-08
19	12	6.7115E-08	−8.2623E-09
19	13	3.3201E-08	−6.3128E-08
19	14	−3.9779E-09	−2.3817E-08
20	13	5.8374E-08	3.3320E-08
20	14	1.1130E-08	−1.6183E-08
21	13	3.6928E-09	−1.6288E-08
21	14	5.2067E-08	3.0801E-10
22	14	−8.0549E-09	2.6440E-08

of the combination solution is given in Figure 4 for $l \geq 6$, where n_l is the number of coefficients of degree l included in the summation. They show a remarkable adherence to the rule of thumb $\sigma_l = 10^{-5}/l^2$.

Figure 5 gives the geoid corresponding to the new combination solution and a flattening of 1/298.258, Figure 6 shows the geoid corresponding to the hydrostatic flattening of 1/299.67, and Figure 7 is a plot of the free-air gravity anomalies corresponding to the combination solution.

Table 4 contains the accuracy estimates of the station coordinates. These estimates are the formal statistics from the combination solution, but, as the subsequent comparisons show, they appear to be realistic.

Figure 8 illustrates the precision estimates of the geoid heights as computed from the precision

estimates of the spherical harmonic coefficients. In this computation, the correlation between coefficients has been ignored because the correlation coefficients are generally less than 0.2. This neglect and the fact that for equal degree and order $\sigma_{C_{lm}}^2 \approx \sigma_{S_{lm}}^2$ mean that the geoid-height precision estimates are essentially longitude independent and symmetric about the equatorial plane. Kozai's accuracy estimates for his zonal harmonics were included in this calculation. Subsequent comparisons with surface gravity and astrogeodetic data show that these precision estimates are quite realistic, and the geoid appears to be determined with an accuracy of 3 to 4 meters. Of course, these accuracy estimates refer to the generalized geoid and do not imply that the geoid is everywhere known with this accuracy. In areas such as the South Pacific, where there are no surface-gravity data and where the gravity field cannot be directly sampled, the uncertainty in geoid height may be larger than the 3 or 4 meters.

Comparison of geometric and dynamic satellite solutions. Figure 9 and Table 6 show the results for the comparisons of the directions computed by the two solutions. The accuracy estimates given by the two solutions are indicated by the error ellipses. The difference δ in

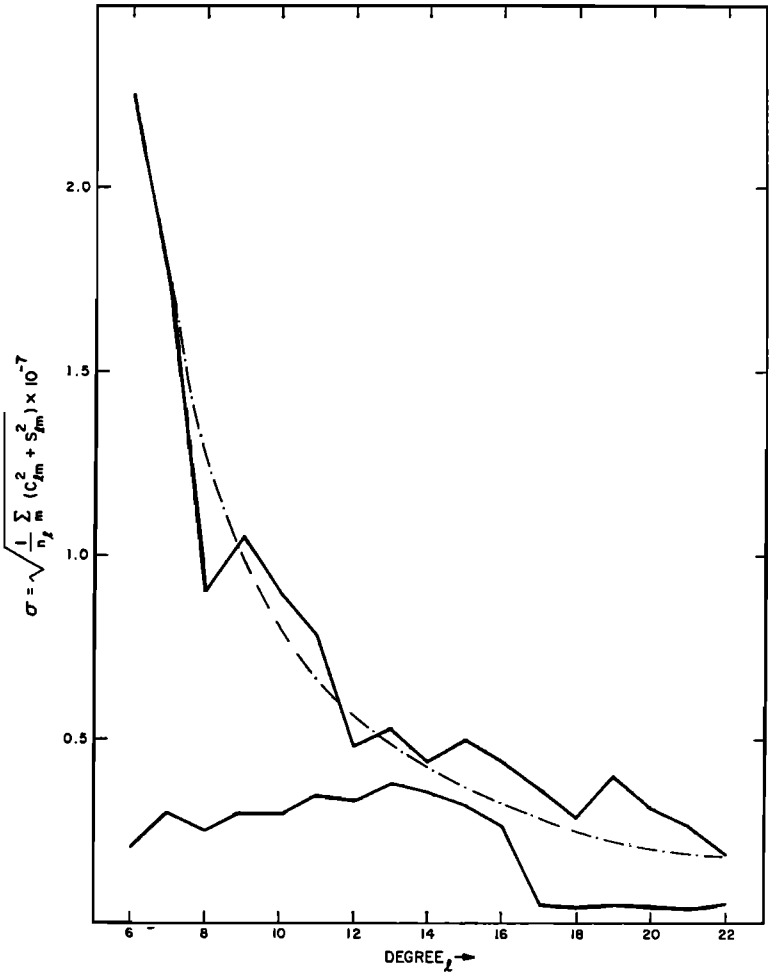

Fig. 4. Power spectrum for $6 < l < 22$ for the combination solution. Kaula's rule of thumb is indicated by the dashed line. For $2 < l < 6$, the spectra are in complete agreement with this rule. The lower curve is the corresponding precision estimates of the harmonics, i.e., $1/n_l \sum_m (\sigma_{C_{lm}}^2 + \sigma_{S_{lm}}^2)$, where n_l is the number of coefficients of degree l included in the summation.

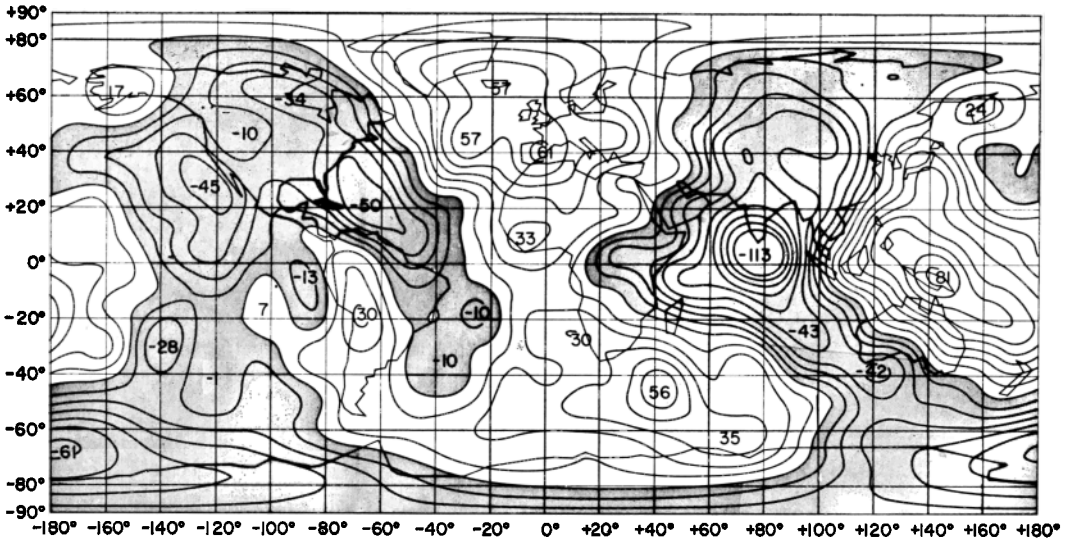

Fig. 5. Geoid heights in meters of the new combination solution corresponding to a reference ellipsoid of flattening $f = 1/298.258$. (Contour interval is 10 meters, and shaded areas are regions of negative geoid height.)

the positions derived from the individual solutions is a good indication of the accuracies that can be expected for the combination-solution coordinates, although it must be pointed out that in Figure 9 the difference between the two solutions results from uncertainties in the coordinates of both stations and that at each station a number of such comparisons can usually be made. Thus, the accuracy of the station positions relative to the origin of the coordinate system should be better than these figures indicate.

The accuracy estimates σ_g of the geometric solution directions are obtained by the method

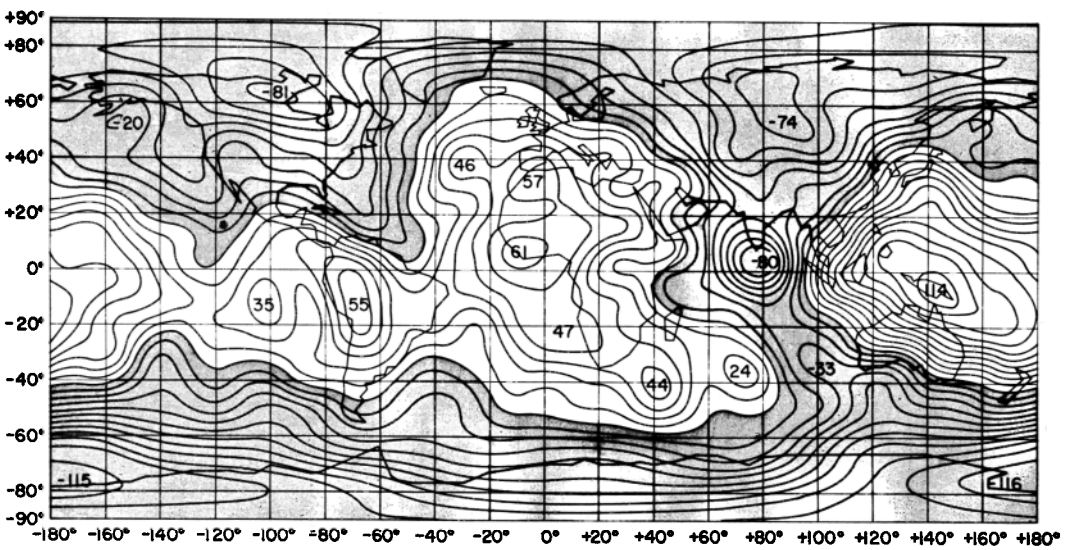

Fig. 6. Geoid heights in meters of the new combination solution corresponding to a reference ellipsoid of flattening $f = 1/299.67$. (Contour interval is 10 meters, and shaded areas are regions of negative geoid height.)

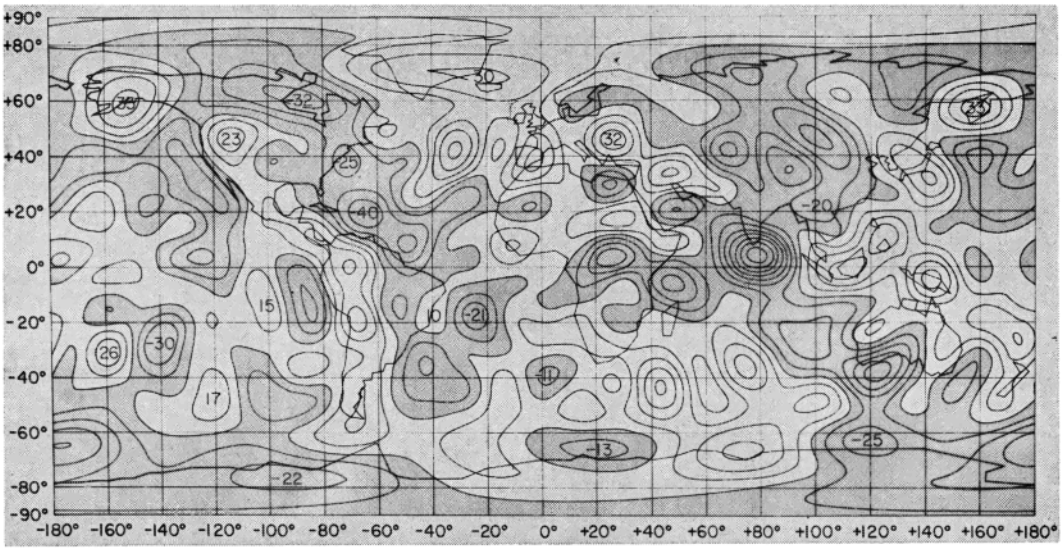

Fig. 7. Free-air gravity anomalies with respect to the best fitting ellipsoid $f = 1/298.258$ from the adopted solution (10-mgal contours; darker shaded areas are regions of negative anomalies).

described earlier. The dynamic solution, however, gives accuracy estimates for the coordinates, and consequently for the station-station vectors σ_D, that are overoptimistic. This is usually evident from figures such as Figure 9, where δ^2 is often considerably greater than either σ_D^2 or σ_G^2. Making an analysis similar to that used in the geometric solution for establishing the accuracy indicates that the covariance matrix of the dynamic solution should be multiplied by a factor of $k_1^2 = 4.5$. When harmonic coefficients derived from different iterations of the dynamic satellite solution are compared, it also appears that the formal variances must be multiplied by a factor of about 5 in order to obtain realistic accuracy estimates.

Figure 9 also indicates the directions of the station-station vector derived from the combination solution compared with the geometric and dynamic results. In view of the above, these comparisons indicate that for the fundamental Baker-Nunn stations (those numbered 9001 to 9012) the combination-solution coordinates should be reliable to better than 10 meters. For the new Baker-Nunn stations (9021, 9028, 9029, 9031, and 9091), from which there are fewer observations, the comparisons indicate that the combination-solution coordinates should be reliable to better than 15 meters. These estimates are in agreement with the formal statistics given in Table 4. The longitude difference between the two satellite solutions obtained from the combination solution is -0.2 ± 0.5 μrad and is not significant.

Comparison with satellite orbits. Each solu-

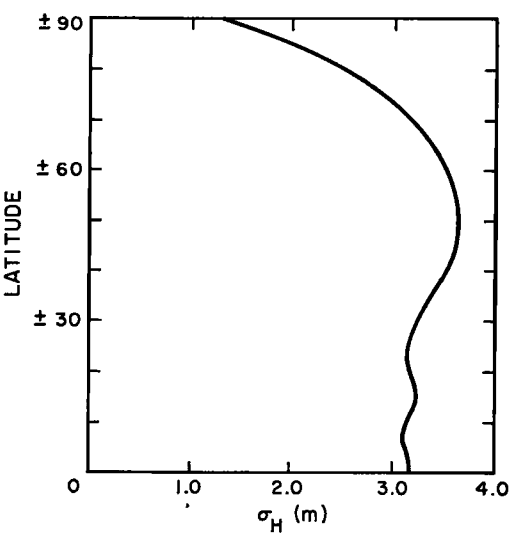

Fig. 8. Precision estimates of geoid heights determined from the harmonic coefficient precision estimates.

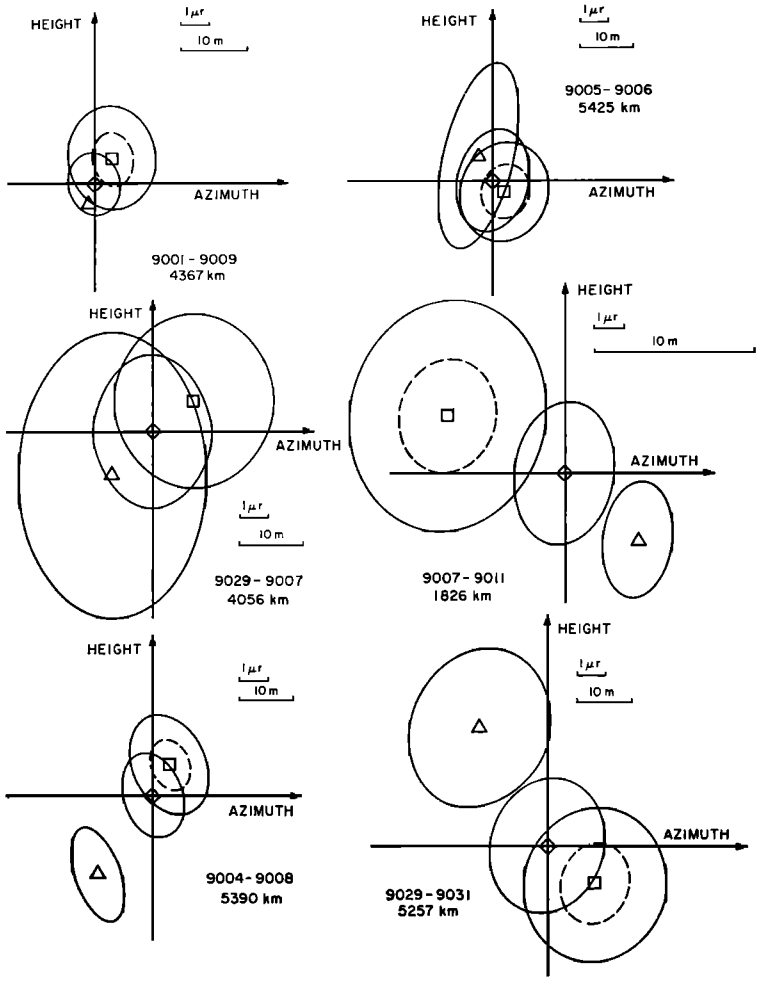

Fig. 9. Comparisons for station-station vectors computed from (triangle) the geometric solution, (square) the dynamic solution, and (diamond) the combination solution. The two error ellipses centered at the square refer to the formal statistics of the dynamic solution (the inner ellipse) and after the covariance matrix has been multiplied by the factor k_1^2 (outer ellipse).

tion resulted in improved orbital residuals; for the final solution, the orbital residuals for satellites such as Geos 1 or Geos 2 are less than 10 meters. These orbits are computed from a combination of laser and Baker-Nunn data for 30 days. The rms residuals for the optical data are 2 arcsec. The laser data have an accuracy of 1 to 2 meters. The rms is 7 meters in all cases, and no residuals exceed 10 meters. These are orbits with significant amounts of laser data from 2 or 3 stations. The 7-meter orbital errors can arise from station-coordinate errors (probably about 5 meters), geopotential errors (possibly 5 meters), and unmodeled periodic perturbations.

Comparison of satellite and deep-space-probe solutions. In order to compare the satellite and JPL solutions, a combination solution using only the satellite and surface-gravity information has been made. Table 7 gives the results for those Baker-Nunn stations that are related to the JPL antennas. From the ground-survey information given by *Gaposchkin and Lambeck* [1970, Table 10], the coordinates for the JPL sites in the SAO system can be computed, and the differences in longitude $\Delta\lambda_i$ and in distance

to the rotation axis Δr_i are given in Table 8. This table also gives the accuracy estimates from the statistics provided by the two solutions and the ground survey. The differences in longitude immediately reflect the systematic longitude differences between the two solutions: the JPL longitudes are to the east of the SAO longitudes. From the over-all combination solution, these transformation parameters are solved for and yield $\langle \Delta\lambda \rangle = -3.2 \pm 0.5$ μrad and $\Delta r/r = (+0.3 \pm 0.5)\ 10^{-6}$, the scale of the SAO system as defined by the station coordinates being larger than that of the JPL system.

The residuals $\langle \Delta\lambda \rangle - \Delta\lambda_i$ and $\langle \Delta r \rangle - \Delta r_i$ are in all cases less than 10 meters and support the accuracy estimates given in Table 4 for stations 9002, 9003, 9004, and 9113. Table 9 gives the adjusted coordinates of the JPL stations in the SAO reference system.

The longitude difference cannot be attributed to the difference in the UT1 time systems used by the two agencies, since at the time of the Mariner 5 observations, UT1(JPL) − UTC = 89.0 msec and UT1(SAO) − UTC = 101.4 msec, so that the expected longitude difference would be +12 msec or 0.8 μrad. The total unexplained longitude difference is, therefore, −4.0 μrad. This discrepancy appears to be due to different definitions of the right ascension of the vernal equinox. At SAO, this is defined by the star positions given in the SAO catalog, which refers to the FK4 system, and at JPL, the vernal equinox is defined in the planetary ephemeris used [*Melbourne and O'Handley*, 1968].

TABLE 6. Summary of Differences δ between Directions Computed from the Geometric Solution with Accuracy σ_G, and from the Dynamic Solution with Accuracy σ_D (μrad)
(k is the factor by which the latter estimates must be scaled.)

Line	σ_G^2	σ_D^2	δ^2	k^2
9001–9009	2.6	0.7	3.2	1.8
9001–9010	2.8	0.9	7.8	4 1
9001–9012	6.5	0.2	3.2	0.9
9002–9028	39.0	1.3	57.8	2.9
9004–9008	4.7	0.7	20.2	7.5
9004–9009	14.1	0.4	25.0	3.3
9004–9010	15.1	0.2	10.9	1.4
9004–9028	9.4	0.8	16.0	3.1
9004–9029	28.9	1.0	51.9	3.5
9005–9006	16.1	0.8	2.6	0.3
9005–9012	61.1	0.6	15.2	0 4
9006–9008	13.5	2.2	6.3	0.8
9007–9009	3.9	1.8	39.6	13.6
9007–9010	2.6	0.5	30.2	18 9
9007–9011	6.8	3.6	60.9	11.7
9007–9029	16.4	2.3	14.4	1.5
9007–9031	17.7	2.1	20.1	2.0
9009–9010	6.5	3.7	18.4	3.6
9009–9011	2.3	0.8	13.0	8.1
9028–9091	23.9	1.5	96.0	7.6
9029–9031	17.7	1.6	44.9	4.6
			k_{av}^2 =	4.9

TABLE 7. Coordinates for Baker-Nunn Stations Derived from a Combination of the Geometric and Dynamic Satellite Solutions and Surface Gravity Only

Station	X, Mm	Y, Mm
9002	5.056126	2.716511
9003	−3.983778	3.743085
9004	5.105587	−0.555230
9113	−2.350466	−4.651977

The scale difference between the two solutions is hardly significant in view of the standard deviation. This would be expected, since both solutions have used the same GM value.

Comparison with surface gravity. To compare the satellite solution with the surface gravity, the following quantities defined by *Kaula* [1966*a*] have been computed:

$\langle g_T^2 \rangle$, mean value of g_T^2, where g_T is the mean free-air gravity anomaly based on surface gravity, indicating the amount of information contained in the surface-gravity anomalies.

$\langle g_S^2 \rangle$, mean value of g_S^2, where g_S is the gravity anomaly derived from the satellite solution, indicating the amount of information contained in the satellite-gravity anomalies.

$\langle g_T g_S \rangle$, an estimate of the mean square of g_H, the true value of the contribution to the gravity anomaly of the estimates of geopotential coefficients from the satellite solution, the amount of information common to the surface-gravity and satellite-gravity anomalies.

$\langle (g_T - g_S)^2 \rangle$, mean square difference of the g_S and g_T.

$E\{\epsilon_S^2\}$, mean square of the satellite error.

$E\{\epsilon_T^2\}$, mean square of the surface-gravity error.

$E\{\delta g^2\}$, mean square of the error of omission, the difference between the true gravity anomaly and g_H.

If the satellite solution gave a 'perfect' estimate

TABLE 8. Results of SAO-JPL Station Comparison
($\Delta\lambda_i$ is the longitude difference and Δr_i is the difference in distance to the earth's axis of rotation for the two solutions. $\langle\Delta\lambda\rangle$ is the weight mean longitude difference.)

Stations	$\lambda_{SAO} - \lambda_{JPL} = \Delta\lambda_i$, μrad	$\langle\Delta\lambda\rangle - \Delta\lambda_i$ μrad	$\langle\Delta\lambda\rangle - \Delta\lambda_i$ m	$\sigma_{\Delta\lambda_i}$ m	$r_{SAO} - r_{JPL} = \Delta r_i$, m	$\sigma_{\Delta r_i}$, m
4751-9002	−3.5	+0 3	+1.9	7.7	+5.9	4.9
4741-9003	−2.2	−0.9	−5.2	6.8	−7.3	4.5
4742-9003	−1.2	−2.0	−10.4	9 0	−6.5	4.5
4761-9004	−4.5	+1.4	+6.9	6.6	−1.2	4.5
4712-9113	−4.9	+1.7	+9.2	12.4	+7.6	5.5

of the C_{lm} and S_{lm}, that is, $\langle g_S^2\rangle = \langle g_H^2\rangle$ ($\equiv \langle g_T g_S\rangle$), then ϵ_S^2 would be zero even though g_S would not contain all the information necessary to describe the total field. The information not contained in the satellite field (the error of omission δg) then consists of the neglected higher-order coefficients. The quantity $\langle(g_T - g_S)^2\rangle$ provides a measure of the agreement between the two estimates g_T and g_S of the gravity field and is equal to the sum of the estimates of the three types of errors. Thus

$$\langle(g_T - g_S)^2\rangle = E\{\epsilon_S^2\} + E\{\epsilon_T^2\} + E\{\delta g^2\}$$

Another estimate of g_H can be obtained from the gravimetric estimates of degree variances σ_l^2 [*Kaula*, 1966*a*]:

$$E\{g_H^2\} = D = \sum_l \frac{n_l}{2l+1}\sigma_l^2$$

where n_l is the number of coefficients of degree l included in g_H. Table 10 gives the σ_l^2 for degree 0 to 16, as well as the degree variances of the satellite and combination solution computed from

$$\sigma_l^2 = \gamma^2(l-1)^2 \sum_m (C_{lm}^2 + S_{lm}^2)$$

If both the satellite solution and the surface gravity gave 'perfect' results for terms up to a given degree, then

$$\langle g_S^2\rangle = \langle g_T g_S\rangle = D \qquad E\{\epsilon_S^2\} = E\{\epsilon_T^2\} = 0$$

Table 11 summarizes the estimates obtained for these quantities from the satellite solution, the combination solution, and the *Gaposchkin* [1966*b*] *M*1 solution. All three sets contain the same zonal harmonics. The estimates are given for three sets of 300-n.mi. squares: (1) the squares for which the number n of observed 60-n.mi. squares is equal to or greater than 1, (2) the squares for which $n \geq 10$, and (3) the squares for which $n \geq 20$. For the last data set, the comparisons are made for the three fields

TABLE 9. Coordinates of the JPL Stations Referred to the SAO Reference System

Station	*X*, Mm	*Y*, Mm	*Z*, Mm
4751	5.085451	2.668252	−2.768728
4741	−3.978706	3.724858	−3.302213
4742	−4.460972	2.682424	−3.674618
4761	4.849242	−0.360290	4.114869
4712	−2.350454	−4.651975	3 665631

TABLE 10. Power Spectra of Free-Air Gravity Anomalies

Degree	Degree Variance, mgal²		
	Gravimetric Solution	Satellite Solution	Combination Solution
0	2.9		
1	−0.2		
2	5.9	7.4	7.4
3	31.0	33.3	33.0
4	18.2	19.7	20.0
5	7.3	17.5	17.8
6	20.7	14 4	15.7
7	9.2	16.4	15.5
8	7.0	8.5	6.7
9	8.7	15.1	12 7
10	9.4	17.7	12.9
11	5.7	13 7	12.2
12	3.5	8.4	5.1
13	7.0		11.1
14	9.4		8.4
15	9.9		13.2
16	5 5		13.8

TABLE 11. Comparison of Satellite and Combination Solutions with Surface-Gravity Measurements (mgal²)

Solution	$\langle(g_T - g_S)^2\rangle$	$\langle g_T g_S\rangle$	$\langle g_S^2\rangle$	D	$\langle g_T^2\rangle$	$E\{\epsilon_S^2\}$	$E\{\epsilon_T^2\}$	$E\{\delta g^2\}$
	$n \geq 1$, N = 935, 300-n.mi. squares							
Combination solution	206	146	225	163	274	79	72	56
Satellite solution	272	110	218	143	274	108	72	92
$M1$ solution	242	90	148	108	274	58	72	79
	$n \geq 10$, N = 369, 300-n.mi. squares							
Combination solution	135	195	230	163	297	35	19	83
Satellite solution	250	127	212	143	297	85	19	151
$M1$ solution	222	102	131	108	297	29	19	176
	$n \geq 20$, N = 136, 300-n.mi. squares							
Combination solution								
$l \leq 8$, $m \leq 8$	165	90	92	102	253	2	11	152
$l \leq 10$, $m \leq 10$	132	119	116	120	253	−3	11	123
$l \leq 11$, $m \leq 11$	135	126	134	126	253	8	11	116
$l \leq 12$, $m \leq 12$	134	129	138	129	253	9	11	113
$l \leq 14$, $m \leq 14$	109	156	166	146	253	10	11	87
$l \leq 16$, $m \leq 16$	75	184	186	163	253	2	11	58
Satellite solution								
$l \leq 8$, $m \leq 8$	179	86	98	102	253	12	11	156
$l \leq 10$, $m \leq 10$	145	109	110	120	253	1	11	133
$l \leq 11$, $m \leq 11$	151	115	126	126	253	11	11	127
$l \leq 12$, $m \leq 12$	163	111	128	129	253	17	11	131
$l \leq 14$, $m \leq 14$	173	117	150	146	253	33	11	125
Total field	177	118	161	143	253	43	11	124
$M1$ solution								
$l \leq 8$, $m \leq 8$	168	85	85	102	253	0	11	157
Total field	168	93	101	108	253	7	11	148

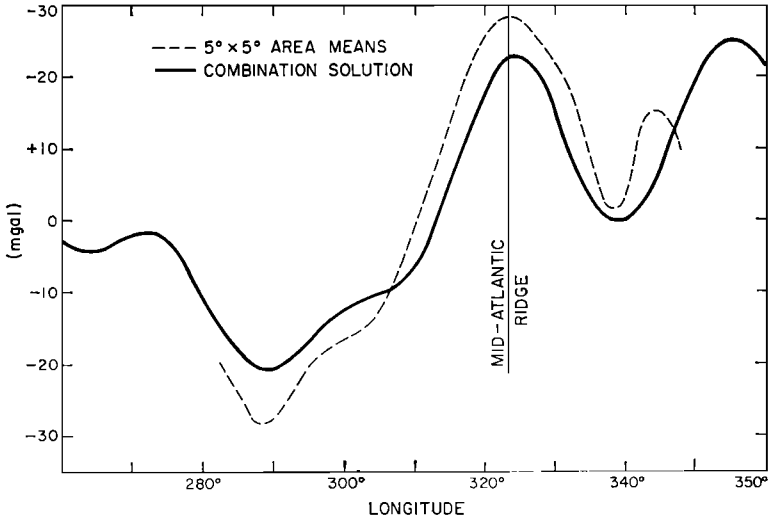

Fig. 10*a*. North Atlantic. $\phi = +32.5°$.

Fig. 10. Comparisons of continuous gravity profiles from shipboard measurements compiled by Talwani and Le Pichon (broken lines) with profiles computed from the combination solution (solid lines).

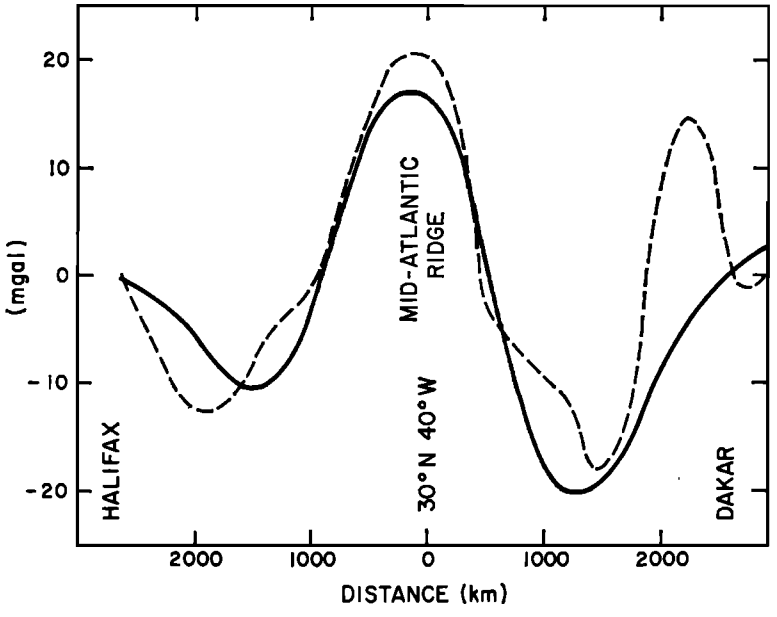

Fig. 10*b*. North Atlantic. NW–SE profile from Halifax to Dakar.

truncated for different degrees, as well as for the total fields.

The variations among the estimates obtained for the three types of errors, $E\{\epsilon_S^2\}$, $E\{\epsilon_T^2\}$, and $E\{\delta g^2\}$, result from the assumptions made about the complete randomness of the quantities g_H, δg, ϵ_T, and ϵ_S.

The combination solution gives the best results in that there is good agreement between the three estimates $\langle g_S^2 \rangle$, $\langle g_T g_S \rangle$, and D of $\langle g_H^2 \rangle$ and

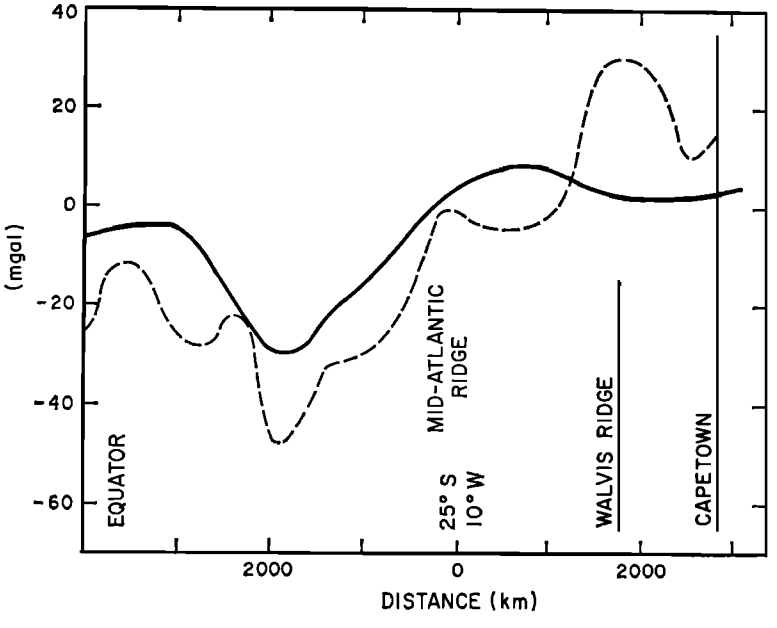

Fig. 10*c*. South Atlantic. NW–SE profile from equator to Capetown.

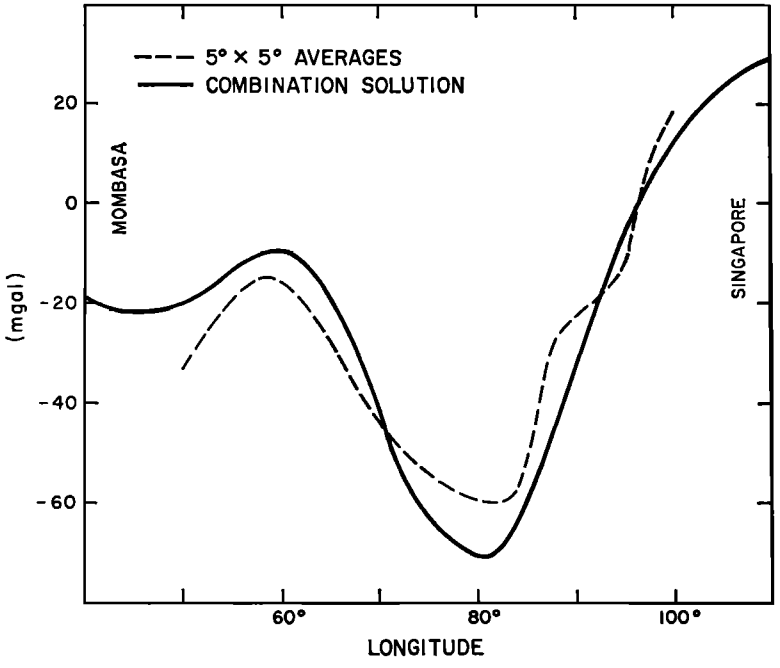

Fig. 10*d*. Indian Ocean. $\phi = 0°$.

the $E\{\epsilon_S^2\}$ and $\langle(g_S - g_T)^2\rangle$ are small. The negative value for $E\{\epsilon_S^2\}$ when $l = 10$ is caused by the combination solution containing the gravity anomalies against which the tests are made. The estimates of the errors of omission are still quite large when compared with the estimates of ϵ_S^2 and ϵ_T^2, indicating that the surface-gravity data have additional information that has not been extracted in this solution.

These tests, however, are not entirely valid

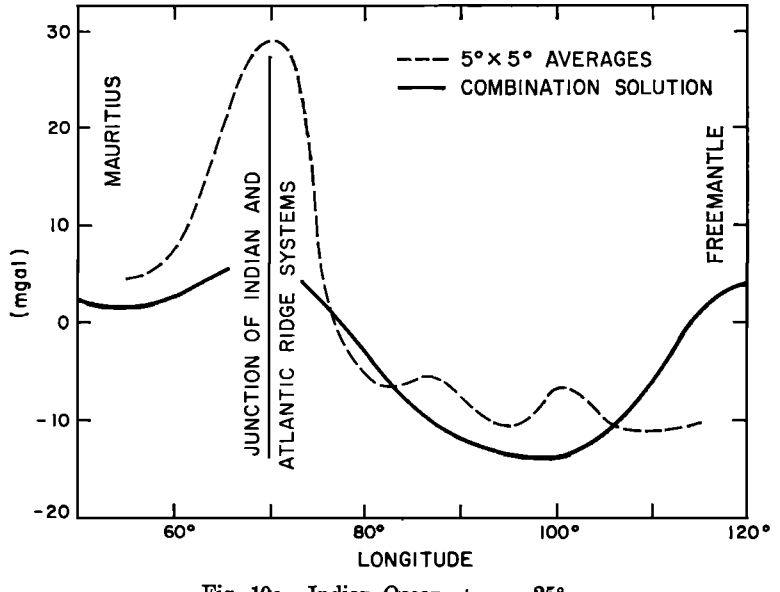

Fig. 10*e*. Indian Ocean. $\phi = -25°$.

TABLE 12. Summary of Comparisons between Surface-Gravity Measurements g_T by Talwani and Le Pichon and Gravity Anomalies g_S Computed from the Combination Solution for Selected Profiles

Profile	$\langle (g_S - g_T)^2 \rangle$, mgal²	$\sigma_{g_T}^2$, mgal²	$\sigma_{g_S}^2 = \langle (g_S - g_T)^2 \rangle - \sigma_{g_T}^2$, mgal²
$\phi = 32.5°$ North Atlantic	84	25	59
NW-SE North Atlantic	68	25	43
NW-SE South Atlantic	222	25	197
$\phi = 0°$ Indian Ocean	80	25	55
$\phi = -25°$ Indian Ocean	166	25	144

$\langle \sigma_{g_S}^2 \rangle = 99$ mgal² ≈ 10 m²

for the combination solution, since the g_H, δg, ϵ_T, and ϵ_S are no longer independent. A better estimate of $E\{\epsilon_S^2\}$ can be obtained from the σ_C, σ_S of the combination solution as indicated by *Lambeck* [1971*b*]. For the total field $E\{\epsilon_S^2\} = 34$ mgal², giving $E\{\delta g^2\} = 30$ mgal². Also, the estimate of $E\{\epsilon_T^2\}$ is likely to be too small, so that $E\{\delta g^2\}$ is even further reduced, and in reality there does not seem to be very much additional information in the surface-gravity data used.

The results obtained from the satellite solution alone are not in such good agreement with the surface-gravity data as is the combination solution. For a gravity field complete to 8, 8, the *M*1 and the new satellite solution give almost equivalent comparisons. For both, the $E\{\epsilon_S^2\}$ are small and there is good agreement among $\langle g_T g_S \}$, $\langle g_S^2 \}$, and D, indicating that the two solutions are equivalent and that they contain most of the information in a 'correct' 8, 8 field. At 10, 10, the new satellite solution shows a marked improvement in the comparison $\langle (g_T - g_S)^2 \rangle$, and this field also appears to be as good as can be expected. But beyond about the 11th order, the comparisons deteriorate and the $E\{\epsilon_S^2\}$ increase.

Further tests with surface-gravity data were made by use of the recent compilations by *Talwani and LePichon* [1969] for the Atlantic Ocean and for the Indian Ocean [*Le Pichon and Talwani*, 1969]. Figure 10 shows free-air grav-

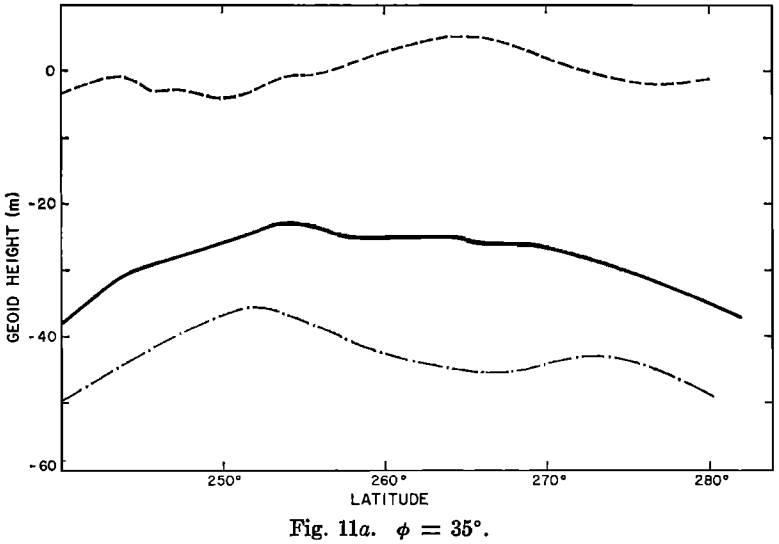

Fig. 11*a*. $\phi = 35°$.

Fig. 11. Comparisons between geoid profiles obtained from the combination solution (solid lines) and profiles obtained from astrogeodetic measurements transformed into the global reference system (dashed lines). The difference between the two profiles, after the systematic part has been subtracted, is shown by the dot-dash lines.

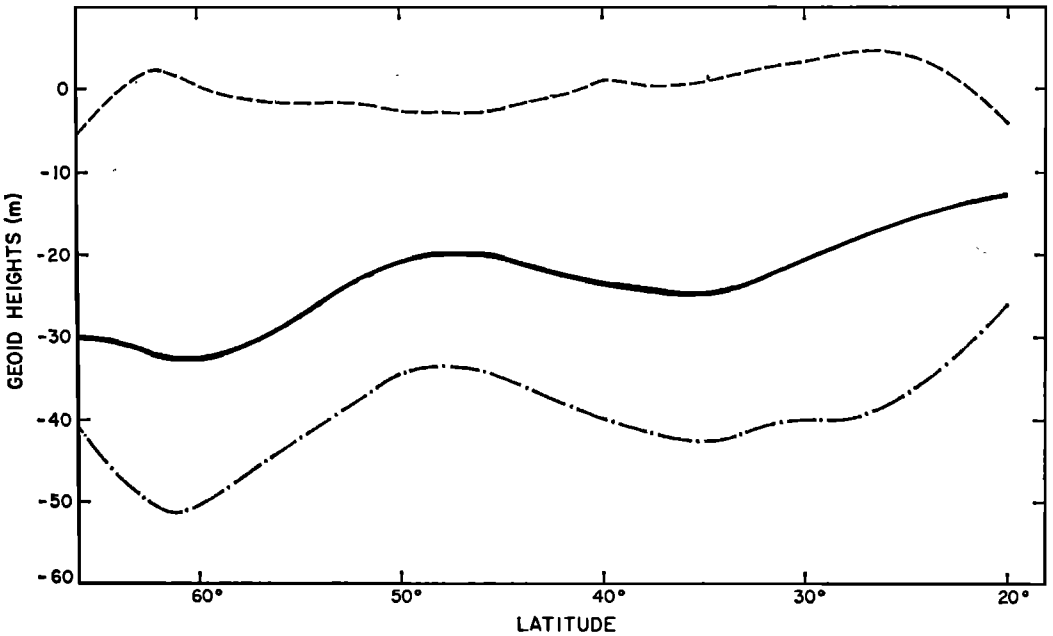

Fig. 11b. $\lambda = 260°$. North American datum.

ity-anomaly profiles computed from 5° × 5° area means from these compilations and from the combination solution. With the exception of the first, these profiles are taken along the ships' tracks where continuous gravity measurements were obtained. The first profile, along latitude 32.5° in the North Atlantic, is midway between two parallel ship cruises. All profiles are referenced to the international gravity formula. The accuracy of the 5° × 5° area means is assumed to be 5 mgal.

Table 12 gives $\langle (g_s - g_T)^2 \rangle$ for each of these profiles, and from these numbers the accuracy of the gravity anomalies computed from the combination solution can be computed. The average value is 10 mgal, or about 3.5 meters in geoid height. This average accuracy estimate is in good agreement with the previous estimates.

Comparison with astrogeodetic data. Geoid heights obtained from astrogeodetic leveling are available for several major datums. These data, like the surface-gravity data, could be used as a further input in the combination solution. However, the coverage extends only to areas where reliable surface-gravity data are also available, and the contribution of the additional information to the global solution is not very significant. Instead, the astrogeodetic data have been used for comparison, thus providing an independent estimate of the accuracy of the global solution.

To compare astrogeodetic geoid profiles with

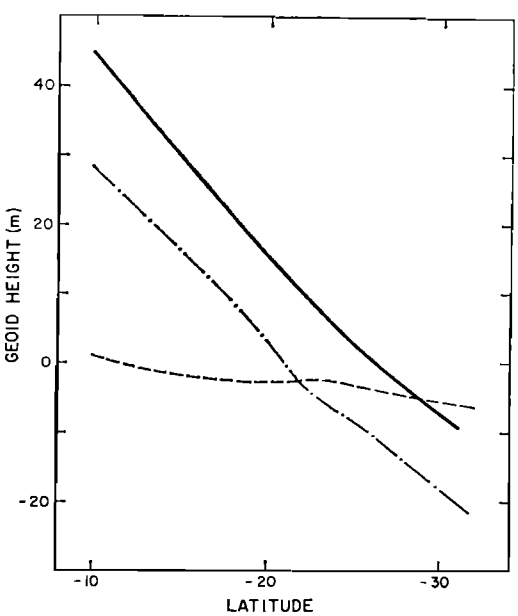

Fig. 11c. $\lambda = 136.25°$.

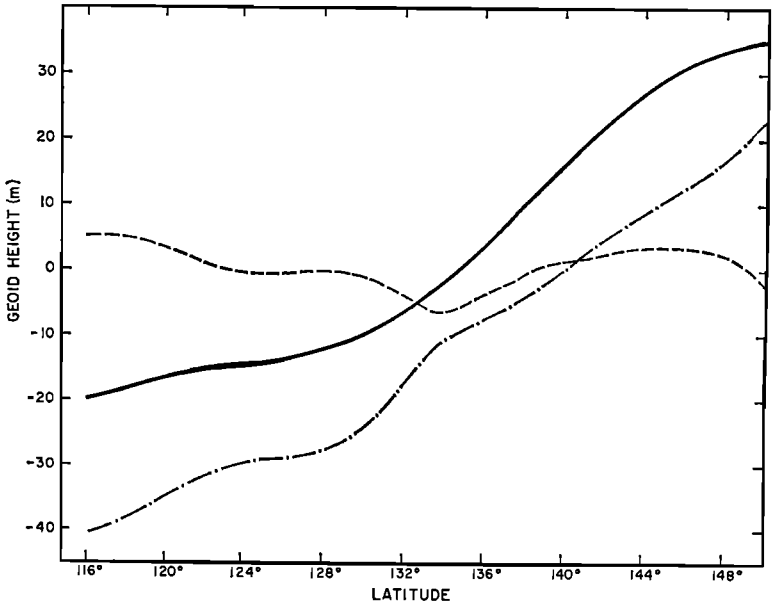

Fig. 11*d*. $\phi = -28.75°$. Australian Geodetic datum.

the global solution, it is necessary that the former refer to an ellipsoid, with its origin at the earth's mass center and of the same dimensions and parallel to the ellipsoid of reference used for the global solution. The transformation elements are given for several major datums by *Lambeck* [1971*a*]. When these transformations contain rotation elements, at least part of the systematic errors in the astrogeodetic heights is absorbed. In the case of the Indian datum, only one station is available for establishing the relationship between the datum and the global solution. Thus only the three translation elements could be determined, and a systematic tilt can be expected.

The following profiles were compared:

1. The geoid section along the 34th parallel in North America given by *Rice* [1962].
2. A section along the meridian of 260° from 65°N to 18°N, selected from the compilation by *Fischer et al.* [1967] for the North American datum (NAD).
3. Two profiles across Australia, one along the latitude circle of −30° and the other along the meridian of 138°, given by *Fischer and Slutsky* [1969].
4. A profile along the meridian of 75° through India [*Survey of India*, 1957].
5. A profile along the meridian of 16° through central Europe [*Fischer*, 1967].

Figure 11 gives the results. All profiles refer to a reference ellipsoid with $a = 6378155$ meters and $1/f = 298.25$. The astrogeodetic profiles are

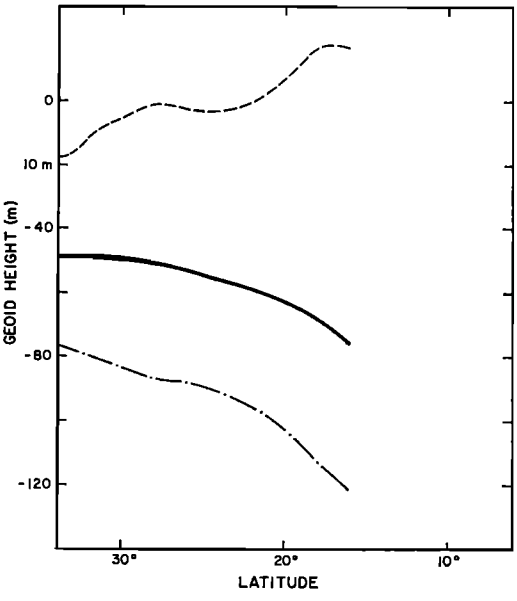

Fig. 11*e*. $\lambda = 75°$. Indian datum.

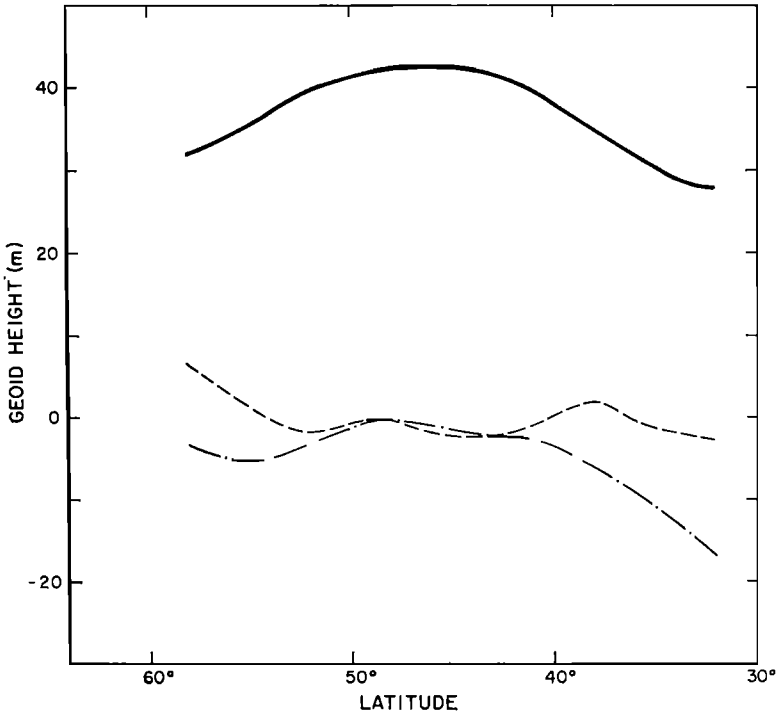

Fig. 11*f*. $\lambda = 16°$. European datum.

smoothed to remove any information with a half-wavelength of less than about 200 km.

The accuracy of the astrogeodetic profiles was assumed to be of the order of 1.5 meters. This is somewhat greater than the accuracy generally stated for this type of observation [e.g., *Bomford*, 1962], but the stochastic nature of the transformation elements also has to be considered.

Table 13 summarizes the results of the comparisons. The average value of σ_S is 3.2 meters and is in agreement with the accuracy estimates derived earlier for the geoid heights of the combination solution.

The negative value for $\langle \Delta h \rangle$ for all the datums considered indicates that the adopted semimajor axis of the reference ellipsoid is too large, by about 15 meters as was noted, for example, by *Veis* [1968]. Figure 11 also suggests a possible tilt in the South Asian datum.

TABLE 13. Summary of the Comparisons between the Geoid Profiles Obtained from the Combination Solution and the Astrogeoids Referred to the Geocentric System
($\langle \Delta h \rangle$ is the systematic height difference between the profiles, $\sigma_{\delta h}^2$ is the variance of the difference between the two profiles, σ_a^2 is the variance of the astrogeoid heights, and σ_S^2 is the contribution of the combination solution to $\sigma_{\delta h}^2$.)

Datum	Profile	$\langle \Delta h \rangle$	$\sigma_{\delta h}^2$	σ_a^2	$\sigma_S^2 = \sigma_{\delta h}^2 - \sigma_a^2$
NAD	$\phi = 35°$	−15	8	1.5	6.5
NAD	$\lambda = 260°$	−16	6	1.5	4.5
AGD	$\phi = -28.°75$	−12	10	1.5	8.5
AGD	$\lambda = 136.°25$	−12	12	1.5	10.5
IND	$\lambda = 75°$	−36	30	1.5	28.5
EUR	$\lambda = 16°$	−42	6	1.5	4.5
					$\langle \sigma_S^2 \rangle = 10.5$ m²

TABLE 14. Results of Differences Δr and Accuracy Estimates $\sigma_{\Delta r}$ between Interstation Distances Computed from the Combination Solution and from Surface Triangulation after Removal of Any Systematic Scale Error in the Datum

Line	$\Delta r \pm \sigma_{\Delta r}$
Comparisons for European Datum	
8015-9004	8.0 ± 9.0
8015-9065	−11.2 ± 9.6
8015-9066	−6.3 ± 3.5
8015-9077	−4.7 ± 10.4
8015-9080	0.1 ± 9.4
8015-9091	−7.1 ± 9.3
8015-9115	22.6 ± 14.8
9004-9065	14.8 ± 12.9
9004-9066	2.3 ± 9.7
9004-9080	−2.9 ± 11.8
9004-9091	3.7 ± 13.9
9004-9115	31.8 ± 18.5
9065-9066	−4.4 ± 9.5
9065-9077	−1.0 ± 13.9
9065-9080	−5.8 ± 10.9
9065-9091	−12.6 ± 13.8
9065-9115	36.4 ± 14.7
9066-9077	−1.2 ± 10.3
9066-9080	−5.6 ± 9.4
9066-9091	−9.1 ± 9.9
9066-9115	27.8 ± 14.2
9077-9080	± 13.4
9077-9091	± 9.8
9077-9115	± 15.3
9080-9091	−15.8 ± 14.9
9080-9115	32.1 ± 14.5
9091-9115	2.1 ± 17.5
Comparisons for North American Datum	
1021-1042	−0.7 ± 7.5
1021-7036	3.5 ± 12.1
1021-7075	−7.0 ± 9.7
1021-9001	−5.6 ± 12.4
1034-7037	3.0 ± 8.9
1034-7045	−1.5 ± 9.9
1034-9010	−1.4 ± 13.0
1034-9113	4.9 ± 12.1
1042-7036	3.4 ± 11.0
1042-9050	15.6 ± 14.2
1042-9114	1.5 ± 17.3
7036-7075	17.3 ± 13.8
7036-9010	4.8 ± 10.3
7037-7045	1.8 ± 9.5
7037-9001	1.6 ± 8.9
7037-9113	1.6 ± 12.1
7045-7075	6.1 ± 13.1
7045-9050	7.1 ± 17.2
7075-9114	−13.7 ± 16.5
9001-9010	6.9 ± 11.7
9001-9050	11.8 ± 17.5
9010-9113	3.1 ± 15.1
9050-9114	−15.2 ± 20.3
9113-9114	14.8 ± 15.7

Comparison with terrestrial triangulation. For stations in North America and Europe, where there are extensive surface triangulation nets, it is possible to compare the coordinates of the tracking stations as determined from the combination solution and from terrestrial measurements. Before a comparison can be made, however, the latter coordinates have to be transferred to a coordinate system coincident with the global geocentric system. These transformations are discussed by *Lambeck* [1971*a*]. For the present solution, the distances between stations are used as the basis of the comparison. These distances are derived from the surface data scaled by the factors determined from the datum adjustments.

Table 14 summarizes the results. The accuracy estimate is computed from the accuracy estimates of the coordinates for the combination solution and from accuracy estimates of the terrestrial data. The latter have been assumed to be reliable to 1 in 200,000.

The first part of Table 14 refers to coordinates in the European datum. All available stations, with the exception of Riga 9074, have been used in this comparison. The second part refers to stations in the NAD. All available stations were used. For most of the comparisons, $\sigma_r > \Delta r$, indicating that the accuracy estimates given for the coordinates of the combination solution (Table 4) are reliable. For station 9115 the agreement is not so good, but it is always within the 3σ level.

Comparison with the 1966 Standard Earth coordinates. Table 15 gives the differences in the coordinates determined in the present solution and in the 1966 solution. For these stations, the accuracy of the latter solution was estimated as 15 to 20 meters, whereas the present solution is considered to be better than 10 meters. With a few exceptions, the differences fall within these limits. The exceptions are stations 9002 and 9003, and the Z component of stations 9007 and 9011. For the first two stations, no comparisons nor combinations could be made in 1966, but a combination and a comparison with the JPL data were possible in this solution and the results are in excellent agreement (Table 8). As for the other two stations, the 1966 geometric solution gave a very weak determination for the Z components because of the poor geometry of the station distribution.

TABLE 15. Differences in Coordinates as Determined in the New Solution and in the 1966 Standard Earth Solution
(Large discrepancies occurred at stations where no comparisons nor combinations of independent solutions were possible in the 1966 solution.)

Station	X, m	Y, m	Z, m
9001	+1.7	−0.6	+1.0
9002	−0.7	+26.0	+32.1
9003	−26.0	−13.8	+26.5
9004	−4.7	+3.7	−7.1
9005	+4.3	+13.4	−11.3
9006	−2.2	+3.3	+8.6
9007	+5.6	−3.4	+27.8
9008	+11.2	−9.0	−4.2
9009	+8.6	−3.6	−4.1
9010	+9.2	−9.2	−2.5
9011	+14.2	−4.0	+30.9
9012	+1.8	−6.8	+0.7
9114	+1.4	+8.4	−8.0
9115	+4.9	+14.6	+5.6
9117	+3.1	+13.9	+4.5

With the relocation of some stations and with more data available, this Z component is determined much better in the present solution and is in good agreement with the results of the dynamic solution. This can be seen from Figure 9 for the line 9007-9029, where the horizontal axis corresponds approximately to the Z axis. For the remaining stations, good comparisons and combinations of the geometric and dynamic solutions were possible in the 1966 solution, and, as a result, these coordinates are not significantly different from the new determination. This stresses the importance of having the two independent techniques to determine the station positions. The similarity of the differences in the Z coordinates for stations 9002, 9003, 9007, and 9011, all of which lie in south latitudes, suggests that the 1966 dynamic solution may have had some systematic biases in it because of a poor distribution of observations in the southern hemisphere.

CONCLUSIONS

1. A combination of the four methods of estimating parameters used in this analysis gives better results than any subset of these methods.

2. The geocentric station positions of the 12 fundamental Baker-Nunn stations and the laser-optical sites at Haute Provence (8015-7815) and Athens (9091-7816) are determined with an accuracy between 5 and 10 meters.

3. To improve upon this accuracy, more laser data for the dynamic solution and laser-optical simultaneous data for the geometric solution are required. An improvement in the knowledge of UT1 is also necessary.

4. The geopotential has been determined complete through $l = 16$, $m = 16$. Comparisons with surface gravity indicate that up to 10, 10 the satellite solution is about as good as can be expected but that some of the higher terms are poorly determined. The terms between degrees 11 and 16 are determined largely from the surface-gravity data. The M1 8, 8 solution is not improved upon by the new solution truncated at 8, 8.

5. Comparisons with independent data sets indicate that the generalized geoid is reliable to about 3 meters.

6. To improve the satellite gravity-field determination for terms beyond $l = 11$, more satellites, in lower orbits, at distinct inclinations, and tracked with greater precision and uniformity, are required.

The numerical results, potential coefficients, and station coordinates can be obtained by writing the authors. In addition, a report detailing the empirical data used and the variance-covariance matrix of the final solution, also available on magnetic tape (upon request), will be issued shortly.

Acknowledgment. This is a condensed review of *Smithsonian Astrophysical Observatory Special Report 315, '1969 Smithsonian Standard Earth (II).'* The work was supported in part by grant NGR 09-015-002 from the National Aeronautics and Space Administration.

REFERENCES

Baarda, W., Statistical concepts in geodesy, *Publ. Neth. Geod. Comm.*, [NS] *2*(4), 1967.

Baarda, W., A testing procedure for use in geodetic networks, *Publ. Neth. Geod. Comm.*, [NS] *2*(5), 1968.

Bomford, G., *Geodesy*, 2nd ed., Oxford at the Clarendon Press, London, 1962.

Cook, A. H., The external gravity field of a rotating spheroid to the order of e^3, *Geophys. J., 2*, 199–214, 1959.

Fischer, I., New pieces in the astrogeodetic geoid map of the world, presented at the 14th General Assembly, IUGG, Lucerne, October 1967.

Fischer, I., and M. Slutsky, A preliminary geoid chart of Australia, *Austr. Surv., 21*, 237–331, 1969.

Fischer, I., M. Slutsky, R. Shirley, and P. Wyatt, Geoid charts of North and Central America, *Army Map Service Tech. Rep. 62*, 1967.

Gaposchkin, E. M., Orbit determination, in *Geodetic Parameters for a 1966 Smithsonian Institution Standard Earth, Smithson. Astrophys. Obs. Spec. Rep. 200,* vol. 1, edited by C. A. Lundquist and G. Veis, pp. 77–183, 1966*a*.

Gaposchkin, E. M., Tesseral harmonic coefficients and station coordinates from the dynamic method, in *Geodetic Parameters for a 1966 Smithsonian Institution Standard Earth, Smithson. Astrophys. Obs. Spec. Rep. 200,* vol. 2, edited by C. A. Lundquist and G. Veis, pp. 105–258, 1966*b*.

Gaposchkin, E. M., A dynamical solution for the tesseral harmonics of the geopotential and station coordinates using Baker-Nunn data, *Space Res., 7,* 683–693, 1967.

Gaposchkin, E. M., Satellite orbit analysis at SAO, *Space Res., 8,* 76–80, 1968.

Gaposchkin, E. M., and K. Lambeck, 1969 Smithsonian Standard Earth (II), *Smithson. Astrophys. Obs. Spec. Rep. 315,* 93 pp., 1970.

Heiskanen, W. A., and H. Moritz, *Physical Geodesy,* W. H. Freeman, San Francisco, 1967.

Kaula, W. M., Tests and combination of satellite determinations of the gravity fields with gravimetry, *J. Geophys. Res., 71,* 5303–5314, 1966*a*.

Kaula, W. M., *Theory of Satellite Geodesy,* Blaisdell Publ., Waltham, Massachusetts, 1966*b*.

Kaula, W. M., Global harmonic and statistical analysis of gravimetry, in *Gravity Anomalies: Unsurveyed Areas,* edited by H. Orlin, pp. 58–67, AGU, Washington, D.C., 1966*c*.

Kaula, W. M., Orbital perturbations from terrestrial gravity data, *Final Report, Contract AF (601)-4171,* 1966*d*.

Köhnlein, W. J., Corrections to station coordinates and to nonzonal harmonics from Baker-Nunn observations, *Space Research, 7,* 694–701, 1967*a*.

Köhnlein, W. J., The earth's gravitational field as derived from a combination of satellite data with gravity anomalies, *Smithson. Astrophys. Obs. Spec. Rep. 264,* 57–72, 1967*b*.

Kozai, Y., Revised values for coefficients of zonal spherical harmonics in the geopotential, *Smithson. Astrophys. Obs. Spec. Rep. 295,* 17 pp., 1969.

Lambeck, K., On the reduction and accuracy of Baker-Nunn observations, in *Reduction of Satellite Photographic Plates,* edited by J. Kovalevsky and G. Veis, *Cospar Trans.,* No. 7, 1969*a*.

Lambeck, K., Position determination from simultaneous observations of artificial satellites: An optimization of parameters, *Bull. Géod.,* no. 92, 1969*b*.

Lambeck, K., The Australian geodetic datum and global satellite solutions, preprint, 1970.

Lambeck, K., The relation of some geodetic datums to a global geocentric reference system, *Bull. Géod.,* no. 99, 37–53, 1971*a*.

Lambeck, K., Comparison of surface gravity data with satellite data, *Bull. Géod.,* in press, 1971*b*.

Lehr, C. G., Geodetic and geophysical applications of laser satellite ranging, *IEEE Trans. Geos. Elec., GE-7,* 261–267, 1969.

Le Pichon, X., and M. Talwani, Regional gravity anomalies in the Indian Ocean, *Deep Sea Res., 16,* 263–274, 1969.

Lundquist, C. A. (Ed.), Geodetic satellite results during 1967, *Smithson. Astrophys. Obs. Spec. Rep. 264,* 344 pp., 1967.

Lundquist, C. A., and G. Veis (Eds.), *Geodetic Parameters for a 1966 Smithsonian Institution Standard Earth, Smithson. Astrophys. Obs. Spec. Rep. 200,* 3 vols., 1966.

Melbourne, W. G., and D. A. O'Handley, A consistent ephemeris of the major planets in the solar system, *Space Programs Summary 37-51,* vol. 3, pp. 4–18, Jet Propulsion Laboratory, Pasadena, California, 1968.

Mottinger, N., Status of D.S.F. location solution for deep space probe missions, *Space Programs Summary 37-60,* vol. 2, pp. 77–89, Jet Propulsion Laboratory, Pasadena, California, 1969.

Rice, D. A., A geoidal section in the United States, *Bull. Géod.,* no. 65, 243–251, 1962.

Survey of India, *Geod. Rep. for 1957,* 1957.

Talwani, M., and X. Le Pichon, Gravity field in the Atlantic Ocean, in *The Earth's Crust and Upper Mantle,* edited by P. J. Hart, AGU, Washington, D.C., 1969.

Tienstra, J. M., *Theory of the Adjustment of Normally Distributed Observations,* N. V. Uitgeverij Argus, Amsterdam, 1956.

Trask, D. W., and C. J. Vegos, Intercontinental longitude differences of tracking stations as determined from radio tracking data, in *Continental Drift, Secular Motion of the Pole, and Rotation of the Earth,* edited by W. Markowitz and B. Guinot, D. Reidel, Dordrecht, Holland, 1968.

Uotila, U. A., Investigations on the gravity field and shape of the earth, *Publ. Inst. Geod. Photog. Cartog., Ohio State Univ., 10,* 92 pp., 1960.

Vegos, C. J., and D. W. Trask, Tracking station locations as determined by radio tracking data, *Space Programs Summary 37-43,* vol. 3, Jet Propulsion Laboratory, Pasadena, California, 1967.

Veis, G., Relation with DSIF stations, in *Geodetic Parameters for a 1966 Smithsonian Institution Standard Earth, Smithson. Astrophys. Obs. Spec. Rep. 200,* vol. 3, edited by C. A. Lundquist and G. Veis, pp. 115–125, 1966.

Veis, G., Geodetic interpretation of the results, *Space Res., 7,* 776–777, 1967*a*.

Veis, G., Results from geometric methods, *Space Res., 7,* 778–782, 1967*b*.

Veis, G., The determination of the radius of the earth and other geodetic parameters as derived from optical satellite data, *Bull. Géod.,* no. 89, 253–275, 1968.

Whipple, F. L., On the satellite geodesy program at the Smithsonian Astrophysical Observatory, *Space Res., 7,* 675–683, 1967.

(Received June 17, 1970;
revised February 18, 1971.)